The ins and outs of photo-assisted microbial electrochemical systems for synchronous wastewater treatment and bioenergy recovery

Yi, Genping; Wang, Bo; Feng, Yufa; Fang, Difan; Yang, Liming; Liu, Wenzong; Zhang, Yifeng; Shao, Penghui; Pavlostathis, Spyros G.; Luo, Shenglian

Total number of authors:
12

Published in:
Resources, Conservation and Recycling

Link to article, DOI:
10.1016/j.resconrec.2022.106230

Publication date:
2022

Document Version
Early version, also known as pre-print

The ins and outs of photo-assisted microbial electrochemical systems for synchronous wastewater treatment and bioenergy recovery

Genping Yi [a, c, 1], Bo Wang [b, d, 1], Yufa Feng [a], Difan Fang [a], Liming Yang [a, *], Wenzong Liu [c], Yifeng Zhang [d], Penghui Shao [a], Spyros G. Pavlostathis [e], Shenglian Luo [a], Xubiao Luo [a, *], Aijie Wang [c]

[a] National-Local Joint Engineering Research Center of Heavy Metals Pollutants Control and Resource Utilization, Nanchang Hangkong University, Nanchang 330063, China

[b] Center for Electromicrobiology, Section of Microbiology, Department of Biology, Aarhus University, 8000 Aarhus C, Denmark

[c] State Key Laboratory of Urban Water Resource and Environment, School of Civil and Environmental Engineering, Harbin Institute of Technology Shenzhen, Shenzhen 518055, China

[d] Department of Environmental Engineering, Technical University of Denmark, 2800 Kgs. Lyngby, Denmark

[e] School of Civil and Environmental Engineering, Georgia Institute of Technology, GA 30332-0512 Atlanta, USA

* Corresponding authors

Tel: +86 73183953371, Fax: +86 73183953373

E-mail: yangliming0809185@126.com (L. M. Yang); luoxubiao@126.com (X. B. Luo).

[1] These authors contributed equally to this work.

Abstract

Wastewater, as the used water, carries huge energy that is frequently ignored and unexploited. Microbes, as bioelectrocatalysts in microbial electrochemical systems (MESs), can convert chemical energy stored in biodegradable matrixes from wastewater to bioelectricity and chemicals. However, due to sluggish wastewater treatment rates and bioenergy production, wider applications have been hampered. Currently, photo-assisted MESs, combined electrochemical/photochemical driving force with microbial catalysis, have emerged as a sustainable platform to enhance pollutants degradation and bioenergy recovery from wastewater with the aid of solar light, accompanied by reasonable energy investment and minimal environmental disturbance. Nevertheless, the development of photo-assisted MESs is still in its infancy. This work broadly concludes present photo-assisted MESs wastewater treatment technologies and their overall limitations in terms of performance and the future advancements that will be necessary to make them more widely applicable. Herein, crucial factors influencing the performance of these photo-assisted MESs, such as the reactor types (bioanode-photocathode, photoanode-biocathode, photomicrobial electrode, and photosynthetic bacteria/algae MESs), the bandgap of semiconductor and microbe species are discussed. Furthermore, prominent research accomplishments of photo-assisted MESs with an emphasis on eliminating contaminants (initial concentration, removal efficiency, and removal rate) and recovering bioenergy (product types, production rate, and current density) from various wastewaters are systematically summarized. Finally, present challenges and prospects in the field of photo-assisted MESs technology are discussed, mainly including the optimization of electrode materials, screening and culture of microorganisms, scale-up of bioreactors,

intermittency of solar energy, and other complications overarchingly shared with photo-assisted microbial electrochemical wastewater treatment and bioenergy recovery.

Keywords: Microbial electrochemical systems; Solar energy; Semiconductors; Electron transfer; Wastewater treatment; Bioenergy recovery

List of abbreviations

COD, Chemical oxygen demand

EAMs, Electrochemically active microorganisms

EDeN, electrotrophic denitrification

EET, Extracellular electron transfer

H_2, Hydrogen

MECs, Microbial electrolysis cells

MESs, Microbial electrochemical systems

MFCs, Microbial fuel cells

MO, Methyl orange

NHE, Normal hydrogen electrode

PEC, Photoelectrochemical cell

PEDeN, Photoelectrotrophic denitrification system

rGO@PPy, Reduced graphene oxide-polypyrrole

3D, Three-dimensional

4-CP, 4-chlorophenol

1. Introduction

The shortage of fossil fuels and increasingly severe environmental pollution have led to a growing demand for sustainable wastewater treatment and energy recovery (Kong et al., 2020; Wang et al., 2014a). Conventional wastewater treatment is confronted with unsustainable issues of intensive energy consumption, high investment cost, and huge greenhouse gases emission (Li et al., 2014b). Meanwhile, valuable resources in wastewater have not been properly recovered, and many additional value-added compounds have not been exploited in conjunction with wastewater treatment (Chu et al., 2020). Microbial electrochemical systems (MESs), which expertly link microbial metabolism with electrochemical processes, have piqued interest in recent decades and opened up new possibilities for simultaneous pollutant removal and bioenergy recovery (Pan et al., 2021).

Electrons in MESs derived from organic wastewater streams can be utilized to generate electricity, hydrogen (H_2), or other value-added chemicals while simultaneously enhancing contaminant removal (Liu et al., 2022; Logan and Rabaey, 2012). The former is referred to microbial fuel cells (MFCs), but large-scale practical applications are restricted due to the low power density and sluggish pollutant removal rates (Slate et al., 2019). The latter is titled microbial electrolysis cells (MECs), while requiring an electric input to induce spontaneous redox reactions, resulting in unsatisfactory economic benefits and operational difficulties (Wang et al., 2020a). Therefore, exploring applicable strategies to effectively improve the overall system performances of MESs, e.g., output voltage, pollutant degradation, and biofuel production, have become a technical bottleneck (Wang and Ren, 2013). Solar energy, as a renewable energy source, is regarded as a promising strategy that could fundamentally address

the above-mentioned issues. The incorporation of solar energy into MESs through semiconductor photoelectrodes and/or photosynthetic bacteria allows the construction of photo-assisted MESs, which is anticipated to improve the overall wastewater treatment performances and also decrease the energy investment of conventional MESs (Fischer, 2018; Weliwatte and Minteer, 2021).

Photo-assisted MESs, which couples semiconductor photoelectrode with bioelectrode, could efficiently overcome thermodynamic energy barriers of MESs and enhance contaminant removal and bioenergy recovery from wastewater (Wang et al., 2014a). Electrons generated by the bioanode flow through the external circuit to interact with the holes produced by the photocathode, when the semiconductor serves as a photocathode. Thus, the recombination of photoinduced electron-hole pairs at the photocathode is effectively retarded by electrons supply from the bioanode and boosts the production of H_2 or multicarbon compounds. Zang et al. reported a bio-photoelectrochemical cell, which was composed of a MoS_3 modified silicon nanowire photocathode and a microbial-catalyzed bioanode, could produce electricity and H_2 under visible light illumination (Zang et al., 2014). Additionally, photosynthetic bacteria could substitute semiconductor photoelectrode to develop analogous photo-assisted MESs (Shukla and Kumar, 2018). On the other hand, a semiconductor photoanode was also combined with the biocathode, where the anodic photoinduced hole can effectively oxidize refractory pollutants and the biocathode can mediate biological wastewater treatment process, e.g., denitrification (Du et al., 2014). Cheng et al. established a photoelectrotrophic denitrification system (PEDeN) with the TiO_2 photoanode and biocathode and greatly achieved nitrate (NO_3^--N) efficient removal solely relying on the illumination without additional chemical reductants

or electric power (Cheng et al., 2017). Previous reviews have presented and discussed the combinations of solar energy and MESs. Wang et al. first reviewed recent accomplishments of solar-assisted MFCs; however, this review mainly focused on bioelectricity or chemical fuel generation (Wang et al., 2014a). In addition, Fischer finitely listed the combinations and classifications of photoelectrical cells and MFCs, but the corresponding applications were not discussed in-depth (Fischer, 2018). Many varieties of photo-assisted MESs have recently been developed and are thus urgently reviewed, more importantly, recent advancements in various prospective applications of wastewater treatment and resource recovery based on the photo-assisted MESs platform are worth concluding fully.

Thus, the objectives of this review are to (i) provide a thorough assessment of existing photo-assisted MESs based on their classifications; (ii) summarize and compare recent advances in photo-assisted MESs for removing organic and inorganic pollutants and recovering bioenergy (such as electricity, H_2, and other value-added biofuels); and (iii) discuss current challenges and future perspectives of the photo-assisted MESs technology for field applications. We anticipate that it will serve as a powerful reference for future efforts to build innovative photo-assisted MESs, investigate multifarious electrode materials and photosynthetic bacteria, produce more diversified MESs products, and possibly industrialize photo-assisted MESs in the near future.

2. Principles and classifications of photo-assisted MESs

In MESs, organic compounds are degraded by exoelectrogenic bacteria while producing electrons and protons in the anode. Then, protons and electrons combine in the cathode to achieve the reduction of electron acceptors. The external voltage could provide the required

energy to improve the overall efficiency and produce H_2; however, it certainly exacerbates the energy consumption (Cheng and Logan, 2007). Solar energy is considered as one of the most viable options, to be introduced into the MES, which could alleviate or avoid dependence on electricity through absorbing and converting light into energy in so-called photo-assisted MESs. Taking semiconductor as the cathode, e.g., MoS_3-modified silicon nanowire photocathode (Zang et al., 2014), the photoelectron potential produced by the semiconductor under illumination can reach about -0.60 V *vs*. normal hydrogen electrode (NHE) (Eq. 1, light wavelength = 420 nm, light intensity = 120 W m^{-2}), which enables cathode H_2 generation since that potential is -0.41 V *vs*. NHE (Eq. 2, pH = 7). When using acetate as the electron donor and oxygen as the electron acceptor, the theoretical anode and cathode potentials calculated by Nernst equation are -0.30 V *vs*. NHE and 0.80 V *vs*. NHE, respectively (Eq. 3 and 4, HCO_3^- = 5 mmol L^{-1}, CH_3COO^- = 5 mmol L^{-1}, pH = 7) (Logan et al., 2006). In addition, the holes generated by the cathode can accept electrons produced from the bioanode, which also greatly improves the degradation efficiency of organic matters by the bioanode.

$$MoS_3/SiNW + hv \rightarrow hv_{VB}^{+} (E_0 = 0.41\ V) + e_{CB}^{-} (E_0 = -0.60\ V\ vs.\ NHE) \quad (1)$$

$$2H^+ + 2e^- \rightarrow H_2 \quad (E_0 = -0.41\ V\ vs.\ NHE) \quad (2)$$

$$2HCO_3^- + 9H^+ + 8e^- \rightarrow CH_3COO^- + 4H_2O \quad (E_0 = -0.30\ V\ vs.\ NHE) \quad (3)$$

$$O_2 + 4H^+ + 4e^- \rightarrow 2H_2O \quad (E_0 = 0.80\ V\ vs.\ NHE) \quad (4)$$

Acknowledgedly, the efficiency of the solar-to-biomass conversion of natural photosynthesis ranges from 2.9% to 4.3% for most crops (Zhang, 2015). By combining with photovoltaic cells to convert natural solar light, it could effectively intermittently regulates (i.e., day-on and night-off powered) bioelectrochemical anaerobic reactor to recover bioenergy from

wastewater (Wang et al., 2020a, b). Another strategy for more efficient photosynthesis is to build a hybrid inorganic-biological system that combines inorganic and microbial assembly (namely photoelectrodes) to synthesis specific chemicals (Zhang, 2015), such as simple compounds like methane and multicarbon compounds, e.g., acetate, n-butanol, polyhydroxybutyrate, and isoprenoids. Various photo-assisted MESs could availably and cheaply improve contaminant removal and harvest bioenergy in a wealth of fields. Thereby, global research on photo-assisted MESs for wastewater treatment and bioenergy recovery has expanded swiftly and advanced in recent years. (Fig. 1A). Diverse photo-assisted MESs configurations (such as bioanode-p-Cu_2O photocathode, TiO_2 photoanode-biocathode, α-Fe_2O_3 photomicrobial electrode, etc.,) emerged, with the representative time nodes illustrated in Fig. 1B. To date, several photo-assisted MESs have been successfully constructed by coupling semiconductor photoelectrodes, solar cells, photosynthetic bacteria, or algae. Solar energy coupling of MESs was utilized in these devices to produce bioelectricity, H_2, and chemical fuels, as well as assistance with pollutants removal (McCormick et al., 2015; Yang et al., 2020). The discovery of these novel photo-assisted MESs provides new insights into the generation of bioelectricity and recovery of bioenergy while removing pollutants from wastewater. Furthermore, these reported novel photo-assisted MESs can be mainly categorized into four types based on the position of photoelectrodes: (i) Type I: bioanode-photocathode MESs; (ii) Type II: photoanode-biocathode MESs; (iii) Type III: photomicrobial electrode MESs; (iv) Type IV: photosynthetic bacteria/algae MESs (Fig. 1C-D).

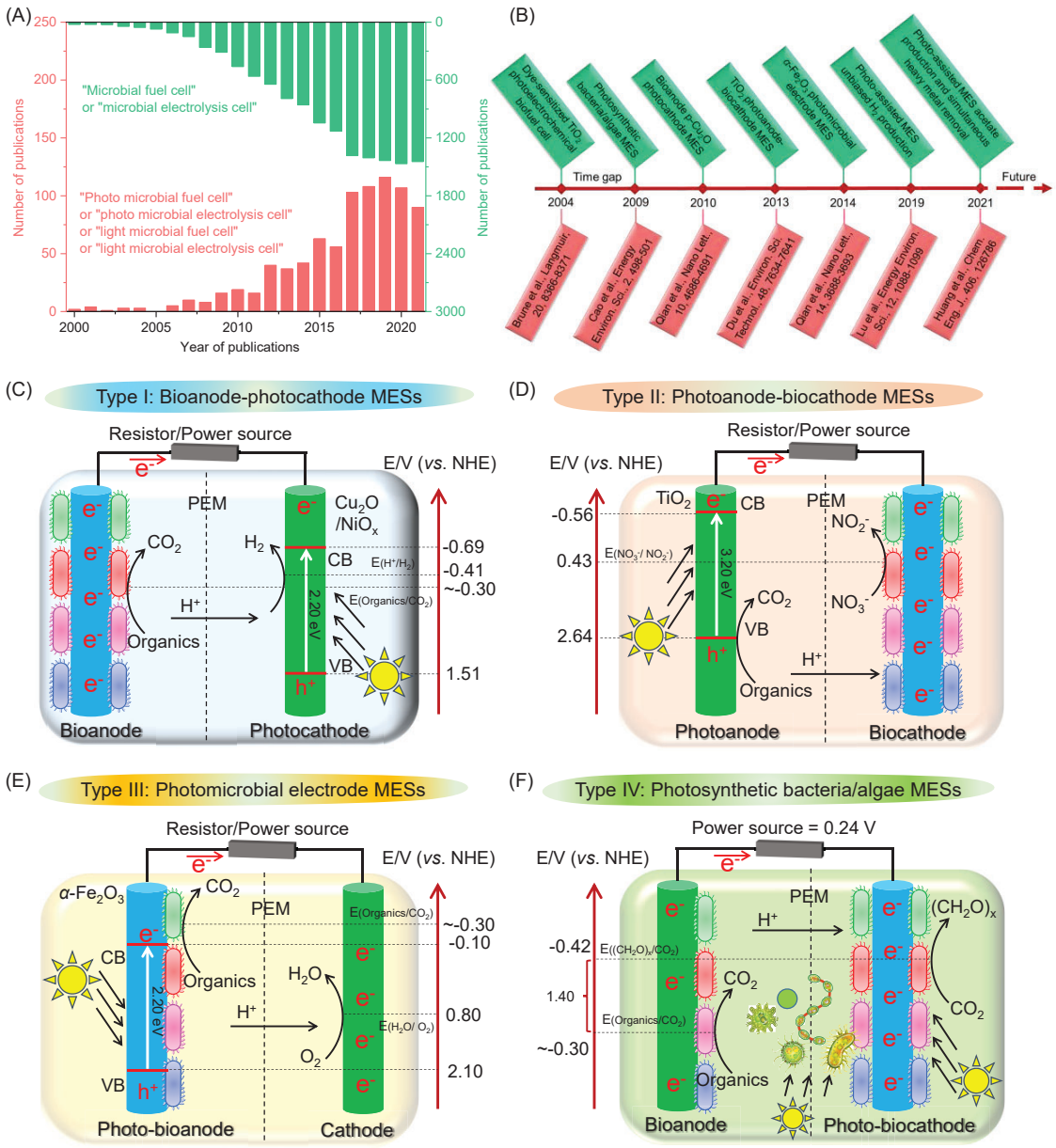

Fig. 1. (A) Numbers of peer-reviewed journal papers on photo-assisted MESs (Numbers based on "Web of science" via searching the keywords: microbial fuel cell, microbial electrolysis cell, photo microbial fuel cell, photo microbial electrolysis cell, light microbial fuel cell or light microbial electrolysis cell; December 2021). (B) Timeline of landmark development in various photo-assisted MESs. (C-F) Classifications and schematic of the photo-assisted MESs, primarily categorized into four types: (C) Type I: bioanode-photocathode MESs; (D) Type II: photoanode-biocathode MESs; (E) Type III: photomicrobial electrode MESs; (F) Type IV: photosynthetic bacteria/algae MESs.

2.1. Bioanode-photocathode MESs

In the bioanode-photocathode MESs (Type I), the bioanode oxidizes organic substrates or pollutants and transmits electrons through the external circuit to the photocathode constituted semiconductor materials (Fig. 1C). Under illumination, the cathode semiconductors are activated to produce electron-hole pairs, which combine vacancies with biological electrons, promoting the electron production rate of anode exoelectrogenic microorganisms, thus increasing the output of current. Matching holes and electrons also accelerates the transition of photogenerated electrons in the semiconductor, which enables more negative photogenerated electrons to participate in cathodic reductive reactions, thus enhancing H_2 or other reduced products production efficiency. Qian et al. reported a microbial photochemical battery driven by solar light, which combined the inorganic photocathode (p-type Cu_2O nanowire-array) with the bacteria-colonized bioanode (inoculated with *Shewanella oneidensis* MR-1), to realize organic matter biodegradation and sustainable energy generation (Qian et al., 2010). The position of the semiconductor band edge associated with the redox potential of bacterial cells is beneficial to the microbially-generated electrons transfer to the semiconductor valence band. Moreover, Zang et al. developed a bio-photoelectrochemical cell with MoS_3 modified silicon nanowire photocathode to accomplish self-sustained H_2 generation (Zang et al., 2014). Therefore, the bioanode-photocathode system deserves further investigation on account of the wide range of processes that can be supported, especially on pollutant degradation and biofuels production.

2.2. Photoanode-biocathode MESs

In the photoanode-biocathode MESs (Type II), a semiconductor serves as the anode for

photocatalysis and electroactive microorganisms act as cathodic catalysts (Fig. 1D). The photogenerated holes at the photoanode under light illumination possess strong oxidation ability, which can effectively and rapidly degrade biorefractory pollutants without the occurrence of secondary pollution. The electrons generated by the semiconductor photoanode are transferred through an external circuit to participate in biocathode reduction reactions. Du et al. employed the holes and/or $^{\bullet}OH$ generated by TiO_2 nanotube arrays photoanode to degrade methyl orange (MO) fast and efficiently (Du et al., 2014). Cheng et al. reported a PEDeN composed of a photoanode and an electrotrophic denitrification (EDeN) biocathode (Cheng et al., 2017). In this device, TiO_2 coated on a Ti sheet acted as a photoanode, while a carbon brush-supported biofilm acted as the biocathode to complete the denitrification process. The EDeN working potential in such a denitrification system was more positive than that of TiO_2, and photoelectrons can be spontaneously generated by the EDeN process. Therefore, different from conventional photoinduced catalysis, nitrogen removal by the PEDeN is completely dependent on the light dose, thereby avoiding additional chemical reductants and energy inputs. The above findings illustrated that the photoanode-biocathode MESs (Type II) were sustainable and environmentally friendly.

2.3. Photomicrobial electrode MESs

Both the bioanode-photocathode and photoanode-biocathode systems partly rely on the external circuit coupling of semiconductors and electroactive bioelectrodes (bioanode or biocathode). However, functional microorganisms and semiconductor materials lack close affiliation in such systems, and thus synergistic effects are not fully realized. In photomicrobial electrode MESs (Type III), electroactive microorganisms are directly attached to the

semiconductor, namely the semiconductor-microbial hybrid electrode, substantially improving the efficiency of photo-assisted MESs (Fig. 1E). Qian et al. reported the interaction between a hematite nanowire-arrayed photoelectrode and *Shewanella oneidensis* MR-1 in a solar-assisted photomicrobial electrochemical system (Qian et al., 2014). The semiconductor holes of the solar-assisted photomicrobial electrochemical system under light can effectively capture electrons and subsequently enhance the oxidative capacity of microorganisms. Meanwhile, the bioelectrons sourced from electrogenic microorganisms combine semiconductor holes, which can produce more photoelectrons to enhance cathodic reduction ability. With a continuous supply of sunlight and organic compounds, the solar-assisted photomicrobial electrochemical system accomplished a self-sustaining manner, which can maintain favorable efficiencies of wastewater treatment, as well as electricity and biofuel generation.

2.4. Photosynthetic bacteria/algae MESs

The photosynthetic bacteria/algae MESs (Type IV) consists of a combination of MES technology and algal cultivation, as an environmentally friendly platform for recovering bioenergy. The anodic photosynthetic bacteria/algae generate electricity via organic compounds oxidization (Fig. 1F). On the other side, the algae cultivated in the cathode chamber enable produce photosynthetic O_2, which could accept electrons from the cathodic reaction, thereby reducing the amount of energy required for aeration. In addition, the algal culture in the photosynthetic bacteria/algae-electrode system could produce valuable by-products, e.g., lipids. Cao et al. unrevealed that direct electron transfer between a cathode and microorganisms for CO_2 fixation in biomass allowed biodegradable organic matters to generate electricity in MESs (Cao et al., 2009). The photocurrent was generated with light-on, while the photocurrent

248 decreased immediately after light stopped, which corroborated the excellent power-generating
249 ability of photosynthetic bacteria. Although photosynthetic MFCs enable renewable energy
250 production, scaling up such systems remains a key issue for photosynthetic bacteria/algae MESs
251 (Type IV) in practice. Yang et al. described a photosynthetic MFC stack made up of multiple
252 anodic chambers that were installed in an algal raceway pond to create a conventional capacitor
253 circuit for recovering biomass energy and power from anaerobically digested wastewater (Yang
254 et al., 2019b).

255 **2.5. Other coupled systems**

256 In addition to the above-described photo-assisted MESs, other coupled systems comprise
257 of various MESs (MFCs or MECs) and/or photoelectrochemical cell (PEC) are also constructed
258 (Type V). For instance, Yuan et al. reported a photo-assisted MES consisting of an air-cathode
259 MFC and a coupled TiO_2-mediated PEC (Yuan et al., 2010). MFC provided external voltage
260 for PEC, which reduced the recombination between photoelectrons and holes, and thus,
261 improved photocatalytic efficiency towards *p*-nitrophenol degradation. Wang et al. further
262 reported self-sustained H_2 production in a PEC-MFC hybrid device, which solely depended on
263 solar light and wastewater (Wang et al., 2013). The PEC-MFC hybrid device was composed of
264 a single-chamber PEC and an air-cathode double-chamber MFC. Under illumination, the holes
265 generated by the TiO_2 photoanode of PEC could oxidize water to oxygen, and the electrons
266 flowed to the MFC cathode to reduce dissolved oxygen. Meanwhile, exoelectrogenic bacteria
267 in the MFC anode oxidized organic compounds to produce electrons. The photovoltage
268 generated by the TiO_2 photoanode shifted the electric potential of the MFC electrodes into more
269 negative, which facilitated electrons generated by the MFC bioanode to reduce protons in the

PEC chamber.

3. Wastewater treatment

Compared to conventional MESs, photo-assisted MESs allow for better anodic oxidation and cathodic reduction under solar energy, resulting in efficient, low-energy wastewater treatment (Fischer, 2018; Wang et al., 2014a). In addition, the photo-induced holes and electrons of semiconductor photoelectrodes also acquire excellent redox capacity, allowing them to degrade persistent contaminants (Qin et al., 2020).

3.1. Organic pollutants removal

Different organic pollutants wastewater can be effectively treated through photo-assisted MESs technology (Table 1, Fig. 2A). Apparently, it is observed that azo dyes, persistent organic pollutants, and biodegradable pollutants account for 36.36%, 31.82%, and 31.82% in organic pollutants removal via photo-assisted MESs, respectively. Additionally, the detailed correlations between the pollutant removal rates and the current density for three organic pollutants were illustrated based on reported studies of photo-assisted MESs (Fig. 2B). It can be found that the maximum removal rate of organic pollutants reached 1105.76 g m^{-3} d^{-1} by the photoelectrocatalytic enhanced MFC (Yuan et al., 2010). Further comparing the average removal rates of organic pollutants by different types of photo-assisted MESs, it could be noted that Type V (other coupled systems) processes the largest removal rate of organics (1105.76 g m^{-3} d^{-1}), while Type II of the photoanode-biocathode MESs has the slowest removal rate (58.34 g m^{-3} d^{-1}) (Fig. 2C). Interestingly, Type I of the bioanode-photocathode MES which has been broadly employed in removing organics from wastewater, accounts for 40.91%, while Type V of other coupled systems accounts for the least (4.55%). In other coupled systems, the

electrochemical process of MFC is similar to that of an external power supply which can provide driven power for the photocatalytic oxidation of organic matters by PEC. The synergistic effect between MFC and PEC greatly increases the pollutants removal efficiency. However, because of the high complexity of this system, the resistance and electrolyte concentration exert a significant impact on its performance. As a result, a sensible design that simplifies the system structure while improving the reactor's operability will become increasingly critical.

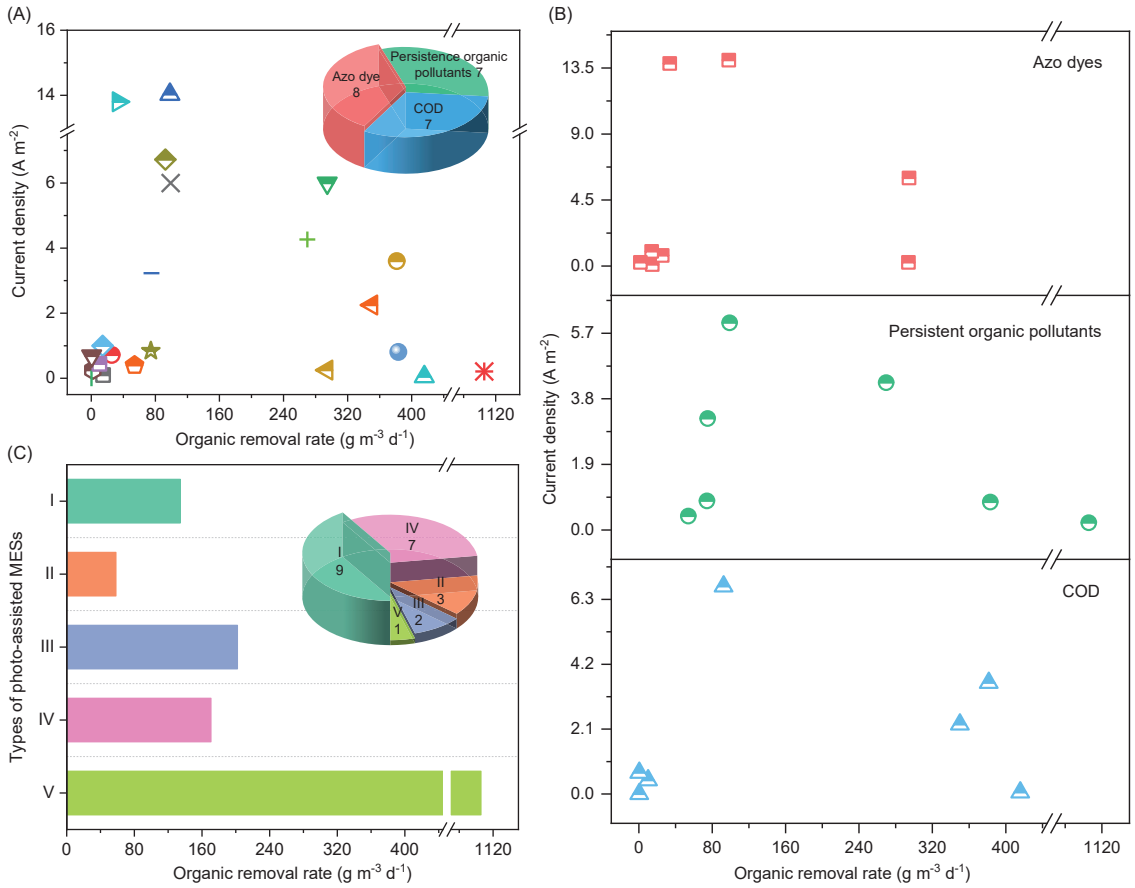

Fig. 2. Photo-assisted MESs for organic pollutants removal from wastewater. (A-B) The relationship between the removal rates of organic pollutants (mainly including azo dye, persistence organic pollutants, and COD) and the current density in various photo-assisted MESs, as well as the type and quantity distribution of organic pollutants (inset). (C) The comparison of organic pollutant removal rates in various photo-assisted MESs, as well as the

corresponding distributions of photo-assisted MESs types (inset). All data is sourced from Table 1.

It has been confirmed that most biodegradable azo dyes can be effectively decolorized in MESs (Mu et al., 2009). However, decolorization is only due to the cleavage of azo bonds (R_1-N=N-R_2), and by-products (such as sulfanilic acid, N, N-dimethylaniline, N, N-dimethyl-p-phenylenediamine) still is a latent threat to the environment (Li et al., 2016b). Many prior studies have revealed photo-assisted MESs can completely degrade or mineralize some azo dyes (Ahmadpour et al., 2020; Sun et al., 2017). Aiming at degrading a typical dye MO, Han et al. reported a bioanode-photocathode MES (Type I) that was composed of a modified p-type Si nanowire photocathode and an exoelectrogen-colonized bioanode (Han et al., 2017). The MO removal rate was enhanced up to 14.08 g m^{-3} d^{-1} by the introduction of photocathode, which can lower the thermodynamic barrier and overpotential of reductive reaction. In addition, photoanode-biocathode MESs (Type II) can achieve faster and more efficient degradation of MO than bioanode-photocathode MESs (Type I). For instance, Du et al. integrated a photoanode with a biocathode and accomplished a MO oxidation rate of 25.53 g m^{-3} d^{-1} (Du et al., 2014). Furthermore, the degradation of persistent organic pollutants (such as phenol and its derivatives) requires a higher energy input due to strong toxicity and low biodegradability. Therefore, photo-assisted MESs can activate TiO_2 semiconductors with energy generated by bacteria and solar energy, thereby effectively degrading phenolic pollutants (Bennani et al., 2015; Wang et al., 2018). Zhou et al. investigated 4-chlorophenol (4-CP) removal in an intimately coupled photocatalysis with biodegradation anode chamber (Zhou et al., 2017). The dechlorination extent of 4-CP was 50%, and the maximum dechlorination rate reached 54 g m^{-3} d^{-1}. Overall, these results showed that the driving power delivered by the microorganisms and

semiconductors could be utilized to enhance the photocatalytic pollutant degradation rate.

In addition, the conventional activated sludge process is widely used for the removal of biodegradable organic pollutants, however, electricity and chemical agents are also required. Recent research has been reported that incorporating photosynthetic bacteria or algae into MESs to construct a photosynthetic algal fuel cell, enables energy production and wastewater treatment without CO_2 emission (Xiao et al., 2012). Xiao et al. designed an integrated algae photo-bioelectrochemical system by installing the MES inside an algal bioreactor (Xiao et al., 2012). During one year of operation, the algae photo-bioelectrochemical cell removed more than 92% chemical oxygen demand (COD), 98% NH_4^+-N, and 82% phosphate, while simultaneously reaching a maximum power density of 1.15 mA m^{-2}. Moreover, Colombo et al. cultivated *Spirulina* in the cathodic compartment of photosynthetic bacteria/algae MESs (Type IV) and the COD removal rate improved to 381.43 g m^{-3} d^{-1} (Colombo et al., 2017).

Together, photo-assisted MESs have outperformed anaerobic digestion in terms of decontamination, particularly in the removal of aqueous resistant contaminants, such as numerous persistent pollutants. This improved performance of photo-assisted MESs may be attributed to the coexistence of anaerobic and aerobic microenvironments, which allows for a wide range of responses that cannot be achieved by anaerobic or aerobic technologies alone. More significantly, photo-assisted MESs can produce high-quality effluent, and algal participation can boost nutrient removal efficiency (nitrogen and phosphate) and biomass production.

348 **Table 1.** Summary of organic pollutants removal from wastewater by photo-assisted MESs and corresponding performance comparison.

Pollutants	Initial concentration ($mg\ L^{-1}$)	Removal efficiency (%)	Reactor types	Anode material	Cathode material	Removal rate [a] ($g\ m^{-3}\ d^{-1}$)	Current density [b] ($mA\ m^{-2}$)	Reference
MO	20	73.4	I	Unpolished graphite	Graphite plate/rutile	14.73	100	(Ding et al., 2010)
MO	4.81	88.31	II	Ti/TiO_2 nanotube arrays	Carbon brush	25.53	716.33	(Du et al., 2014)
MO	50	98	I (0.8 V)	Graphite brush	Ni foam/TiO_2	98.2	14030	(Hou et al., 2017b)
MO	50	97.8	I (0.8 V)	Graphite brush	g-C_3N_4/BiOBr	294.6	6000	(Hou et al., 2017a)
MO	25	84.5	I	Carbon felt/granular graphite	Pd-modified silicon nanowire	14.08	1000	(Han et al., 2017)
Congo red	300	98	IV	AQDS/Mn/PPy	AQDS/Mn/PPy	294	250	(Sun et al., 2017)
Brilliant red X3	10	85	I	Graphite granules	Titania nanotube arrays	33.72	13800	(Long et al., 2019)
Reactive black 5	10	55.56	I	Graphite plate	AgBr/CuO modified graphite	1.85	250	(Ahmadpour et al., 2020)
Phenol	20	62	II	TiO_2/Ti	Graphite plate	74.35	840	(Bennani et al., 2015)
4-CP	24.68	90.5	III	Carbon foam/N-TiO_2	Stainless steel mesh	54	400	(Zhou et al., 2017)
Ethyl acetate	125	~100	I	Graphite particles/rod	PVDF/carbon cloth/TiO_2	383.28	810	(Wang et al., 2018)
Acid orange 7	50	90.97	I (0.6 V)	Carbon brush	BiOBr	269.75	4266.67	(Qin et al., 2020)
Nitrofurazone	50	83.14	I (0.7 V)	Carbon brush	g-C_3N_4/CdS	99.07	6000	(Hou et al., 2020)
p-nitrophenol	319.95	90	V	TiO_2 (P25)	Carbon paper	1105.76	210	(Yuan et al., 2010)
Pyridine	150	~100	II	$BiVO_4$/FeOOH	NA[c]	75.15	3230	(Shi et al., 2020)
COD	266.7	92.43	IV	Carbon brush	Pt/C	0.52	1.15	(Xiao et al., 2012)
COD	1000	92.1	IV	Graphite felt/microalgae	Carbon cloth/Pt	10.17	444.43	(He et al., 2014)
COD	3000	89	IV	Carbon cloth	Activated carbon/PTFE	381.43	3600	(Colombo et al., 2017)
COD	270	61.6	IV	Carbon brush	Carbon cloth/activated carbon	415.8	49.29	(Luo et al., 2018)
COD	204.6	93.2	IV	Carbon brush	Carbon brush	0.49	689.66	(Wang et al., 2019)
COD	6000	88.6	IV	Carbon brush	Carbon cloth	92.5	6720	(Yang et al., 2019b)
COD	350	82.2	III	Polydimethylsiloxane	NA	350	2250	(Zhang et al., 2020)

349 Notes: a. Calculation based on the reactor volume with available data; b. Calculation based on the electrode area with available data; c. Not
350 available.

3.2. Inorganic pollutants removal

A variety of inorganic pollutants wastewater can be effectively treated through photo-assisted MESs technology. By classifying these inorganic pollutants, we can find that heavy metals, denitrification, and desalination account for 35.00%, 35.00%, and 30.00%, respectively (Fig. 3A). In addition, the detailed correlations between the pollutant removal rates and the current density for three inorganic pollutants were illustrated based on reported studies of photo-assisted MESs (Fig. 3B). According to photo-assisted MESs classification for inorganic matter removal, the photomicrobial electrode MESs (Type IV) accounts for about 45% at most, while photoanode-biocathode MESs (Type II) only accounts for 10%. Furthermore, the fastest average removal rate is also from the photosynthetic bacteria/algae MESs (Type IV, up to 66339.26 g m^{-3} d^{-1}), implying that the systems have enormous potential for inorganic matter removal (Fig. 3C).

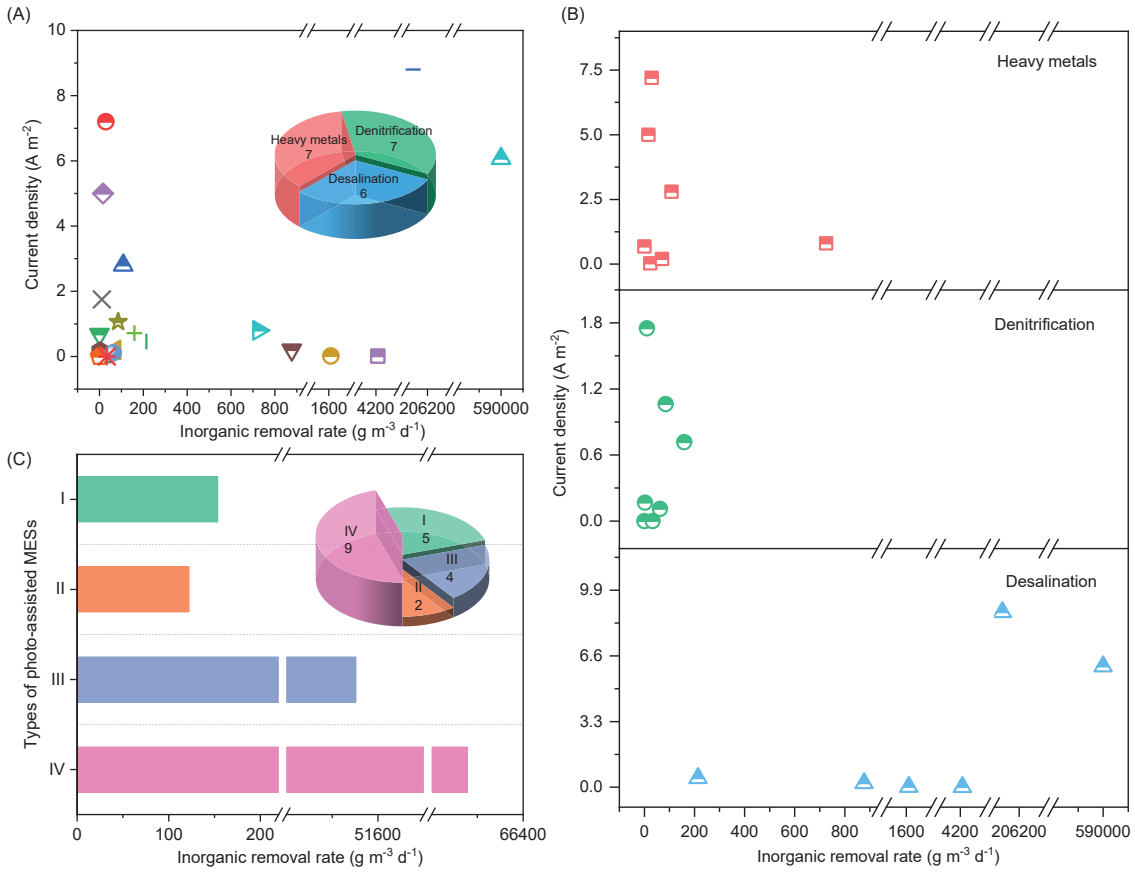

Fig. 3. Photo-assisted MESs for inorganic pollutants removal from wastewater. (A-B) The relationship of the removal rates of inorganic pollutants (mainly including heavy metals, denitrification, and desalination) and the current density in various photo-assisted MESs, as well as the type and quantity distribution of inorganic pollutants (inset). (C) The comparison of the removal rates of inorganic pollutants in different photo-assisted MESs and the corresponding distributions of photo-assisted MESs types. All data is sourced from Table 2.

Emerging photo-bioelectrochemical technology provides a new perspective for efficient metal ions recovery, due to its flexible platform for redox-oriented processes. The advantage over traditional metal treatment, for example, is that the photo-assisted MESs are energy-saving and chemicals-free (Huang et al., 2021). Ren et al. reported a silicon solar cell equipped with double anodes, which consisted of a conventional carbon felt bioanode and one-dimensional TiO_2/Fe_2O_3 photoanode (Ren et al., 2018). The improvement of TiO_2/Fe_2O_3 response

performance to visible light owed to the formation of a heterogeneous structure, which was biocompatible with most bacterial communities and enhanced the treatment ability of metal-containing wastewater. The modified photomicrobial electrode MES (Type III) achieved 90.9% removal of Cr(VI), and the removal rate reached 29.12 g m^{-3} d^{-1} (Table 2). Zhang et al. introduced photosynthetic algae (*Chlorella sp.* QB-102) microalgae on NF/rGO cathode for Cd(II) removal in photosynthetic bacteria/algae MES (Type IV), which achieved a high Cd(II) removal efficiency of 95% and a maximum removal rate of 70.26 g m^{-3} d^{-1} (Zhang et al., 2018a). Photo-assisted MESs are greatly utilized in these studies to remove or transform heavy metals from wastewater, further research directions on the systems are required to achieve high-value-added metal ions recovery (Yang et al., 2022a).

Several typical inorganic water pollutants, such as NO_3^--N, phosphate, and salt ions also can be removed by photo-assisted MESs. Generally, NO_3^--N is commonly removed through biological processes, which requires large amounts of organic matter (as electron donors) to overcome a low C/N ratio and achieve biological denitrification (Lin et al., 2017). Recently, Cheng et al. first applied denitrification biocathode coupling of TiO_2 photoanode to effectively reduce NO_3^--N (Cheng et al., 2017). Under UV illumination, TiO_2 photoanode provided electrons for an external circuit through water electrolysis, and NO_3^--N acts as an electron acceptor for the biocathode. At the end of the batch test, NO_3^--N was almost completely converted to N_2 with a removal rate of 85.26 g m^{-3} d^{-1}. Furthermore, a sustainable bioelectro-photocatalytic nitrate-reducing system was developed (Lin et al., 2017), in which NO_3^--N was the electron acceptor in a bacteria-catalyzed cathode. Interestingly, by the remaining photoelectrons, NO_3^--N was completely reduced to N_2 at a rate of 2.71 g m^{-3} d^{-1} without external

voltage supplied (Table 2); no toxic nitrite or ammonium accumulated throughout the process. Moreover, Liang et al. reported a high-performance photomicrobial desalination cell based on photo-electrochemical interactions (Liang et al., 2016b). The salt removal extent by the photomicrobial desalination cell always kept higher than 96% and the removal rate reached 206.13 kg m^{-3} d^{-1}. Compared with traditional denitrification processes, bacteria in the photo-assisted MESs can directly utilize electrons that are generated in the photochemical process for denitrification without consuming additional chemical reducing agents or electricity. This cleverly revealed that photo-assisted MESs play a positive role in the nitrogen cycle in the water environment. Desalination, unlike the removal of heavy metals and total nitrogen, does not entail an oxidation-reduction process, thus making it easier for occurrence. Cations and anions undergo directional migration with the assistance of an electric field. Moreover, desalination reactors are primarily flow devices, and therefore accelerating mass transfer would greatly boost the reaction rate. Barahoei et al. built a high-performance chemical photosynthesis desalination cell, and the desalination rate reached up to 590 kg m^{-3} d^{-1} and a current density of 6.07 A m^{-2} (Barahoei et al., 2021).

413 **Table 2.** Summary of inorganic pollutants removal from wastewater by photo-assisted MESs and corresponding performance comparison.

Pollutants	Initial concentration mg L^{-1}	Removal efficiency %	Reactor types	Anode material	Cathode material	Removal rate [a] (g m^{-3} d^{-1})	Current density [b] (mA m^{-2})	Reference
Cr(VI)	26	97	I	Unpolished graphite plate	Polished graphite/rutile	23.4	28.57	(Li et al., 2009)
Cr(VI)	50	90.9	III (0.6 V)	Graphite felt/TiO_2/Fe_2O_3	Polished graphite	29.12	7200	(Ren et al., 2018)
Cr(VI)	120	90	III	Carbon rods	WO_3/MoO_3/g-C_3N_4	108.17	2800	(Zhang et al., 2018b)
Cr(VI)	20	99.57	I	Graphite plates	MoS_2/TiO_2	0.11	680	(Shan et al., 2020)
Cr(VI)	40	~100	I	Carbon felt	Ti_3AlC_2	16	5000	(Yang et al., 2022b)
Cd(II)	50	95	IV	NF/rGO	NF/rGO	70.26	200	(Huang et al., 2021)
Cu(II)	200	90.7	I	Carbon brush	$BiFeO_3$/ZnO	725.6	800	(Lam et al., 2022)
NO_3^--N	15.5	60	I	Carbon paper	TiO_2 nanoparticles P25	2.71	166.67	(Lin et al., 2017)
NO_3^--N	35	97.02	II	TiO_2/Ti plate	Graphite granules	85.26	1062.5	(Cheng et al., 2017)
NO_3^--N	39	90	IV	Carbon cloth	Carbon cloth	0.04	0.11	(Kokabian et al., 2018b)
NH_4^+-N	314	~100	IV	Nickel foam	Nickel foam	62.5	110	(Sun et al., 2019)
NH_4^+-N	78	34	II	Ti/TiO_2 nanotube arrays	Carbon brush	159.12	716.33	(Du et al., 2014)
NH_4^+-N	80	78	IV	Carbon brushes	Carbon cloth	10.4	1750	(Luo et al., 2020)
NH_4^+-N	50	94.05	III	Carbon rod	TiO_2/Co-WO_3/SiC	33.19	0.16	(Sun et al., 2020a)
Desalination	40000	96.63	III	Graphite flake/α-Fe_2O_3	Graphite felt	206133	8800	(Liang et al., 2016b)
Desalination	9900	30.30	IV	Carbon papers	Carbon papers	214	460.56	(Kokabian and Gude, 2015)
Desalination	35000	33.4	IV	Carbon cloth	Carbon cloth	4208.82	12.19	(Arana and Gude, 2018)
Desalination	35000	32.2	IV	Carbon cloth	Carbon cloth	1610	15.61	(Kokabian et al., 2018a)
Desalination	12000	69	IV	Al	Carbon felt	590000	6070	(Barahoei et al., 2021)
Desalination	20000	65.8	IV	Graphite plate	Graphite plate	877.33	202.2	(Bejjanki et al., 2021)

414 Notes: a. Calculation based on the reactor volume with available data; b. Calculation based on the electrode area with available data.

4. Bioenergy recovery

MESs, as a sustainable platform, greatly integrate microbial metabolism with electrochemical processes to achieve bioenergy production. Nevertheless, low power output efficiency is the main obstacle towards scalable applications. Despite the fact that investing in higher external voltage to drive MESs can overcome thermodynamic barriers, however, introducing semiconductors or photosynthetic bacteria with solar energy to MESs is deemed as an ecologically benign and sustainable strategy. In the following section, recent research on photo-assisted MESs for electricity recovery, H_2 generation, and chemical fuel production is comprehensively summarized.

4.1. Electricity

Generally, exoelectrogenic microorganisms degrade organic compounds (such as acetate, glucose, polysaccharides, cellulose, etc.,) to produce electrons in the anode, which are then transferred to the cathode through the external circuit, and then the bioelectricity can be generated. However, power produced by traditional MFCs is relatively low and tricky to use. In the photo-assisted MESs, due to the cooperation of cathode and semiconductor, electron holes are generated under light, which promotes the transfer of anode electrons to the cathode, thereby enhancing electrical energy output. Besides the cathode, the anode also is closely related to bacterial attachment and extracellular electron transfer (EET) and affects the power output performance (Guo et al., 2017; Guo et al., 2019). On the basis of high efficiency, designing simple and cost-effective photo-assisted MESs tends to be of significance in terms of productivity. A single-chamber photoanode-biocathode MES (Type II) was constructed via utilizing TiO_2 nanotube array anode and a bilirubin oxidase biocathode, displaying a great

improvement in biofuel cell performances and achieving a maximum power density of 18.5 A m^{-2} with an open-circuit voltage of 1.0 V (Han et al., 2012). Besides, to improve the microbial EET rate, that is the MESs electricity generation efficiency, Feng et al. developed a photo-bioanode that combined carbon material with an α-Fe_2O_3 photocatalyst, utilizing visible light to accelerate biofilm formation and EET in MESs (Feng et al., 2016). The start-up time was cut in half in the photomicrobial electrode MES (Type III), and the maximum current density (8.4 A m^{-2}) was almost twice that of a bioelectrochemical cell in dark (4.0 A m^{-2}) (Fig. 4). The current density of the photo-bioelectrochemical cell showed almost no decrease after being subjected to 40 d of illumination. The electrical energy generation capability of photo-assisted MESs has substantially increased as a result of ongoing research, resulting in a breakthrough in the broad development of MESs (Zhu et al., 2017). Furthermore, Feng et al. obtained an ultra-high current density of 46.5 A m^{-2} by constructing a three-dimensional (3D) carbon-coated stainless steel felt bioactive side and a flat α-Fe_2O_3-coated stainless steel plate photoactive side (Feng et al., 2018). The synergistic effect of photocatalysis and microbial electrocatalysis is an effective method to improve the electricity yield of performance 3D MESs anode. When further analyzing the types of photo-assisted MESs in terms of electricity generation, it could be found that the photomicrobial electrode MESs (Type III) account for as much as 32.43%. Moreover, the photoanode α-Fe_2O_3 coupled *Shewanella* bacteria account for more than 50% in Type III (Table 3). This shows the excellent photoelectric effect and biocompatibility of α-Fe_2O_3, as well as provides new perspectives for searching specific biocompatible semiconductor materials.

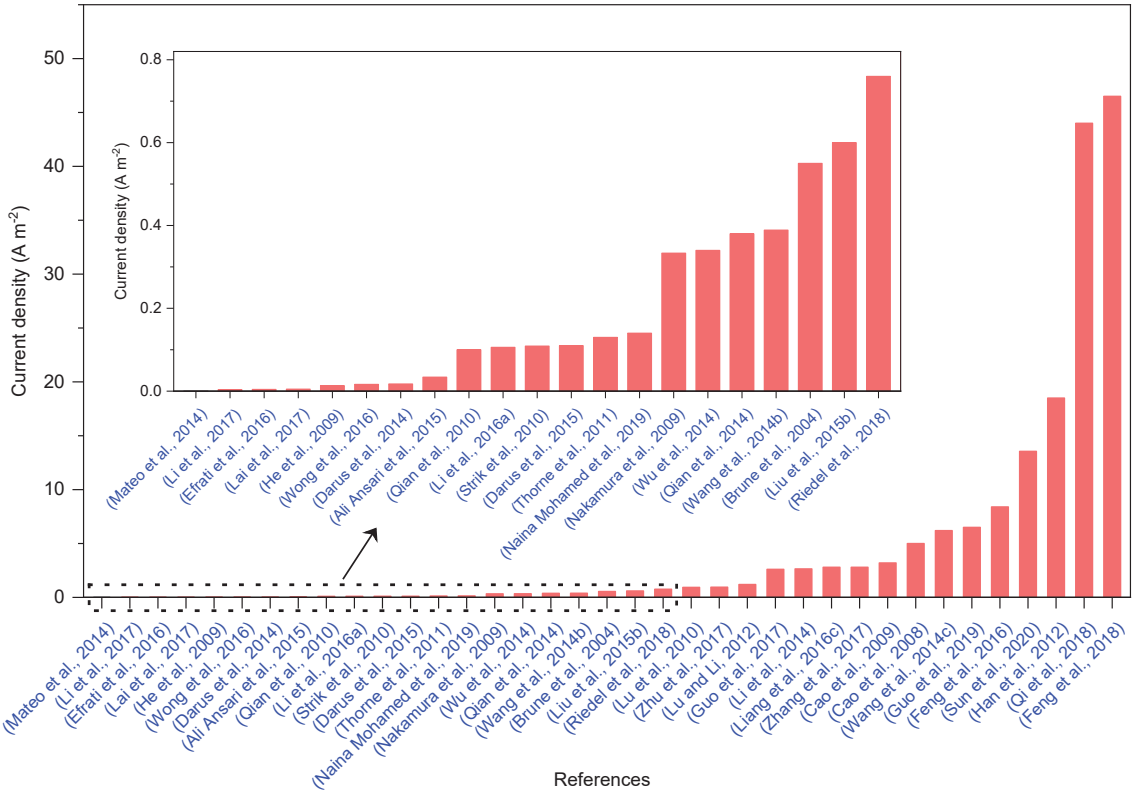

Fig. 4. Comparisons of the current generation in different photo-assisted MESs.

459 **Table 3.** Summary of electricity recovery from wastewater by photo-assisted MESs and corresponding performance comparison.

Pollutants/substrates	Reactor types	Anode material	Cathode material	Current density [a] ($mA\ m^{-2}$)	Reference
Glucose	III	FTO/TiO_2	Hg/Hg_2SO_4	550	(Brune et al., 2004)
Sodium acetate	IV	Graphite felt	Graphite felt	5000	(Cao et al., 2008)
Organic matters	IV	Round graphite felt	Graphite plate	13.33	(He et al., 2009)
Lactate	III	OM c-Cyts/α-Fe_2O_3	Pt	333.33	(Nakamura et al., 2009)
Sodium acetate	I	Graphite	Graphite/rutile	933.35	(Lu et al., 2010)
Organic matters	IV	FTO/TiO_2 ceramic	Activated carbon cloth	130	(Thorne et al., 2011)
Trypticase soy broth	I	Carbon	p-type Cu_2O nanowire	100	(Qian et al., 2010)
Sodium acetate	I	Unpolished plain graphite	Rutile	1200	(Lu and Li, 2012)
Glucose	II	TiO_2	BOD/CNTs-IL/GCE	18500	(Han et al., 2012)
CO_2	IV	Graphite plate	Stainless steel grid	0.008	(Mateo et al., 2014)
Sodium acetate	IV	Carbon felt	Titanium wire	13555.55	(Sun et al., 2020b)
Acetate/fumarate	III (0.2 V)	α-Fe_2O_3/ITO	Pt	2647.66	(Li et al., 2014a)
Lactate/fumarate	I	Carbon granules	$CuInS_2$	6200	(Wang et al., 2014c)
CO_2	IV	Graphite felt	Titanium wires	110	(Darus et al., 2015)
Broth/lactate	I	N-doped graphene sponge	p-type CuS	2607	(Guo et al., 2017)
Sodium acetate	III (-0.2 V)	Stainless steel/α-Fe_2O_3	Graphite felt	2800	(Liang et al., 2016c)
Organic matters	III (0.25 V)	PSII/$(TiO_2)_5$-NTs/ITO	Pt	106	(Li et al., 2016a)
Organic matters	III (0.25 V)	ITO/PPyBQ/PSII	Platinum wire	3.6	(Li et al., 2017)
Glucose	III	PQQ/PSI/$Os^{2+/3+}$/GO_X	Pt plate	4.25	(Efrati et al., 2016)
Acetate	III (0 V)	Graphite plate/α-Fe_2O_3	Graphite felt	8400	(Feng et al., 2016)
Sodium D-lactate	III	Hematite nanowire array	Platinum plate	950	(Zhu et al., 2017)
Organic matters	II	Zn-doped hematite/FTO	BOD/GCC	2800	(Zhang et al., 2017)
Sodium acetate	III (-0.2 V)	Stainless steel/α-Fe_2O_3/carbon	Carbon felt disc	46500	(Feng et al., 2018)
Organic matters	III (0.69 V)	IO-TiO_2|PbS|POs|PSII	IO-ATO|PC|BOD	760	(Riedel et al., 2019)
Luria-Bertani broth/lactate	I	N-doped graphene aerogel	Cu_2O/Au nanowire	6500	(Guo et al., 2019)

Sodium acetate	I	Carbon paper	PtO_x@M-TiO_2 and PtO_x@P-TiO_2	34	(Ali Ansari et al., 2015)
Potassium acetate	IV	Graphite felt	Graphite felt	109	(Strik et al., 2010)
Sodium acetate	IV	Graphite felt	Graphite felt	340	(Wu et al., 2014)
Sodium acetate	IV	Carbon fiber brushes	Carbon felt coat Pt	600	(Liu et al., 2015b)
Luria-Bertani medium	IV	Platinum wire	Glassy carbon electrode	16.5	(Wong et al., 2016)
Acetate	IV	Graphite plate	Graphite plate	140	(Naina Mohamed et al., 2019)
Organic matters	IV	Carbon felt/stainless steel	Carbon felt/stainless steel	44000	(Qi et al., 2018)
Sodium acetate	IV	Carbon cloth	Carbon cloth/PTFE/Pt	5	(Lai et al., 2017)
Sodium acetate	IV	Plain graphite felt	Plain graphite felt	3200	(Cao et al., 2009)
Trypticase soy broth	III (0.8 V)	α-Fe_2O_3	Pt	380	(Qian et al., 2014)
Organic matters	IV (0.6 V)	Graphite felt	Titanium mesh	17.5	(Darus et al., 2014)
Glucose	IV	TiO_2	Graphite	389	(Wang et al., 2014b)

Notes: a. Calculation based on the electrode area with available data.

461 **4.2. Value-added chemicals**

462 Extensive research efforts have been directed towards the development of photo-assisted
463 MESs for various value-added chemicals production with semiconductor photocathodes.
464 Different biofuels (including H_2 and chemicals) can be effectively produced. According to
465 statistical analysis of existing literature, H_2 accounts for 62.5%, and other chemicals including
466 acetate, formate, isopropanol, lipid, and methane can account for 37.5%, respectively (Fig. 5A).
467 The Cu_2O/NiO_x composite photocathode efficiently extracted excited electrons, and the
468 maximum H_2 production rate of 291.2 mmol L^{-1} h^{-1} was obtained under continuous light
469 illumination with 0.2 V external voltage (Fig. 5B) (Liang et al., 2016a). For chemical fuels
470 generation, Liu et al. demonstrated that a hybrid semiconductor nanowire bacteria system with
471 only solar energy input can reduce CO_2 at neutral pH to a wide array of chemical targets, with
472 acetate production rate as high as 1.2 g L^{-1} d^{-1} (Fig. 5C) (Liu et al., 2015a).

473 H_2 as a promising clean energy carrier, yet is hindered by its production in traditional
474 MESs (particularly MECs) due to thermodynamic barriers for cathode proton reduction and
475 anode organic oxidation, thus, the additional exterior voltage needs to be added, integrated
476 sustainable solar energy may be a substituted choice (Lu et al., 2017). Chen et al. employed an
477 n-type TiO_2 nanorods array as the photocathode, which overcame the thermodynamic barrier
478 of H_2 production (Chen et al., 2013a). The maximum H_2 production rate was 7.86 mmol L^{-1} h^{-1}
479 under the condition of light instead of direct current. Furthermore, Liang et al. fabricated a
480 Cu_2O/NiO_x hybrid photocathode by spin coating a thin film of NiO_x on a Cu_2O photocathode
481 to improve its stability and photocurrent (Liang et al., 2016a). However, the anodic oxidation
482 cannot well match the cathodic reduction in MESs. To address this drawback, Lu et al.

483 demonstrated the self-sustained bioanode-photocathode MESs (Type I), which coupled
484 microbial electrochemical oxidation with photo-electrochemical water reduction for H_2
485 generation (Lu et al., 2017). Notably, the microbial photosynthesis system showed a stable and
486 continuous H_2 production efficiency under solar illumination, with a rate of 0.35 mmol L^{-1} h^{-1}
487 within 24 h (Table 4). Giving practical wastewater treatment applications, Lu et al. reported a
488 superior performance photo-assisted MESs, consisting of bioanode and black silicon
489 photocathode with a unique "Swiss-cheese" interface (Type I) (Lu et al., 2019). Semiconductor
490 materials with light illumination generated energy instead of external voltage input, the
491 microbial photo-electrochemical system attained H_2 production up to 1.08 mmol L^{-1} h^{-1} (Table
492 4), and its stability has been maintained for more than 90 h with a high Faraday efficiency (96
493 - 99%). The advent of semiconductors allows for unbiased H_2 generation from applied voltage to
494 photo-assisted MESs, resulting in revolutionary progress in H_2 production. However, the durability
495 and stability of the system require further investigation, and plenty of efforts are needed to realize
496 industrial-scale production (Zeng et al., 2020). Also, seeking cheap, suitable valence bandwidths
497 semiconductor materials is fiercely urgent.

498 Compared with H_2, liquid chemical fuels have attracted widespread attention due to their
499 higher energy density, wider network distribution, as well as well-established storage facilities
500 (Cai et al., 2020). Cao et al. developed a completely anoxic photosynthetic bacteria/algae MESs
501 (Type IV) that fed with bicarbonate as electron receptors and firstly verified the possibility of
502 direct electron transfer between the cathode and microorganisms for CO_2 fixed in biomass
503 under lighting conditions (Cao et al., 2009). Liu et al. reported a novel solar-powered generation
504 of high value-added chemicals by combining semiconductor nanodevices with bacterial

biocatalysts (Liu et al., 2015a). In this process, a biologically compatible array of light-capturing nanowires was designed to directly interact with microbial systems. This hybrid semiconductor nanowires bacterial system driven by solar light could reduce CO_2 to a wide range of targeted chemicals, such as fuels, polymers, and complex drug precursors. For example, in an aerobic (21% O_2 v/v) atmosphere, photoelectrochemical acetate was produced at a high rate of 1.2 g L^{-1} d^{-1} (Table 4). Torella et al. developed a microbial-inorganic integrated photosynthetic bacteria/algae MES (Type IV), where bacterial species *Ralstonia eutropha* was employed to effectively convert CO_2 into biomass and alcohols (Torella et al., 2015). The equivalent solar-to-biomass yield reached 3.2% exceed that of most terrestrial plants, and the *Ralstonia eutropha* employing process resulted in a yield rate of 0.04 g L^{-1} d^{-1} fusel alcohol isopropanol from CO_2. Furthermore, Li et al. developed a novel airlift type photosynthetic bacteria/algae MESs (Type IV) using *Chlorella vulgaris*, which achieved the maximum CO_2 fixation rate, lipid productivity, and current density in the system, respectively, of 1292.8 mg L^{-1} d^{-1}, 0.23 g L^{-1} d^{-1}, and 441.75 mA m^{-2} (Li et al., 2019). Microalgae also exhibit a high growth rate and a strong ability to capture and utilize CO_2. The direct production of high value-added chemicals using CO_2 and H_2O through photo-assisted MESs is a process that simulates natural photosynthesis, which is of practical importance. As a sustainable solar-driven CO_2 emission reduction platform, the photo-assisted MESs will receive further attention. However, the system still encounters many problems, such as the slow synthetic rate of chemical substances and the low purity of products. Despite the numerous hurdles that remain to be overcome, photo-assisted MESs have demonstrated their enormous ambition as novel alternative technologies in environmental remediation, where pollutants removal performance and energy recovery are the

primary design objectives.

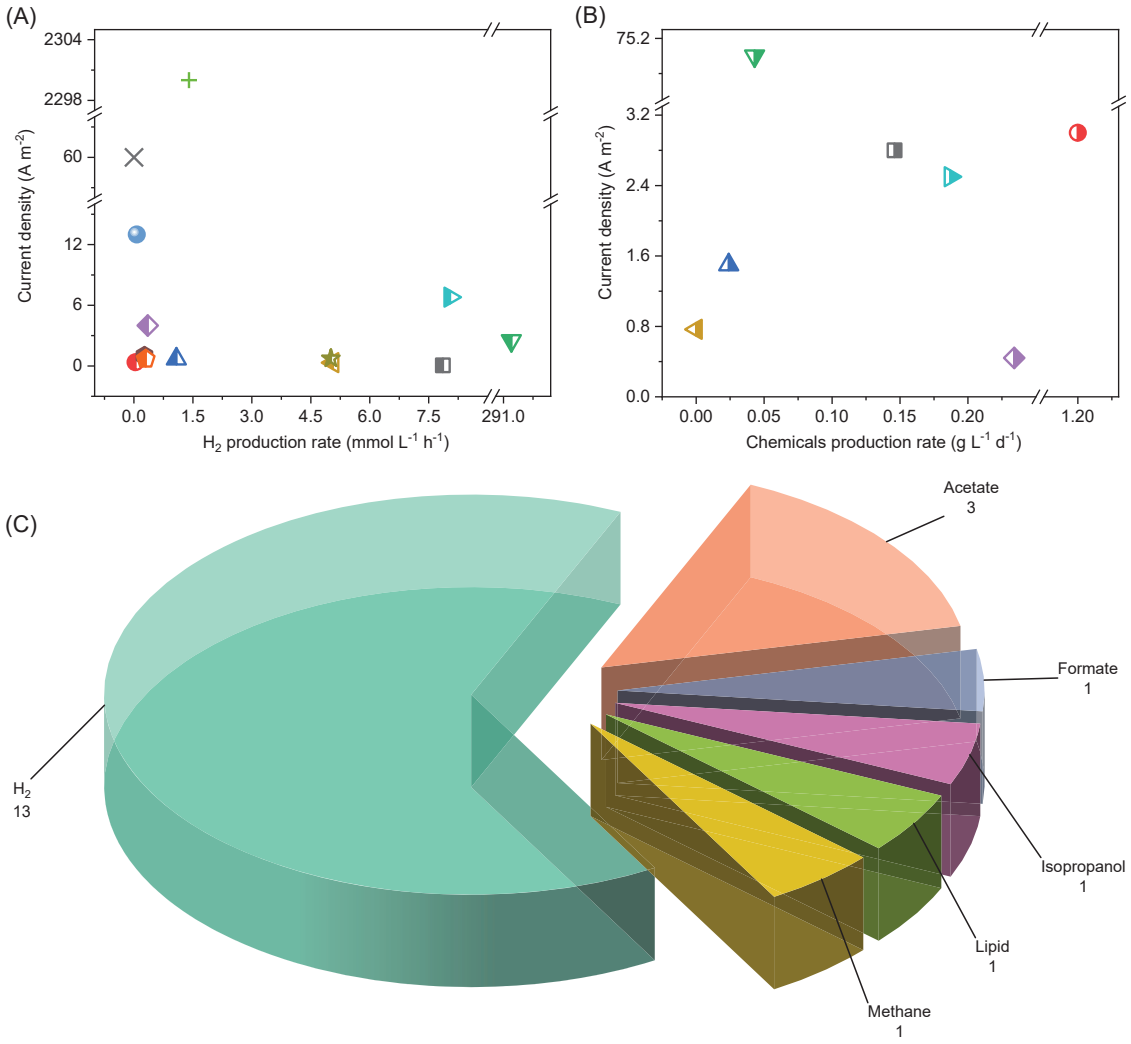

Fig. 5. Photo-assisted MESs for bioenergy recovery from wastewater. (A) The relationship of H_2 production rates and the current density in different photo-assisted MESs. (B) The comparison of the production rates of chemicals and the current density in different photo-assisted MESs. (C) The proportion of different biofuels production in the photo-assisted MESs.

Table 4. Summary of value-added chemicals production from wastewater by photo-assisted MESs and corresponding performance comparison.

Pollutants/ substrates	Reactor types	Products	Anode material	Cathode material	Production rate [a]	Current density [b] ($mA\ m^{-2}$)	Reference
Acetate	I	H_2	Carbon brush/Ti wire	Nanostructured n-type TiO_2	7.86 mmol L^{-1} h^{-1}	55	(Chen et al., 2013a)
Organic matters	IV	H_2	Carbon paper	Pt	0.04 mmol L^{-1} h^{-1}	370	(Chen et al., 2013b)
Acetate	I	H_2	Graphite felt	MoS_3/p-type Si nanowire	1.08 mmol L^{-1} h^{-1}	690	(Zang et al., 2014)
Sodium acetate	I	H_2	Graphite felt	Cu_2O/NiO_x	291.2 mmol L^{-1} h^{-1}	2500	(Liang et al., 2016a)
Sodium acetate	I	H_2	Carbon brush	$GaInP_2/TiO_2/MoS_x$	0.35 mmol L^{-1} h^{-1}	4000	(Lu et al., 2017)
Acetate	I	H_2	Carbon cloth	MoS_2/Cu_2O	5.06 mmol L^{-1} h^{-1}	322.92	(Jeon et al., 2018)
Sodium acetate	I	H_2	Graphite rod/carbon felt	MoS_2/PDA/TiO_2	8.04 mmol L^{-1} h^{-1}	6800	(Zeng et al., 2019)
Organic matters	V	H_2	TiO_2	FTO	0.27 mmol L^{-1} h^{-1}	1000	(Chae et al., 2009)
Acetate	V	H_2	Pt	$WO_3/NiFe_2O_4$	5.01 mmol L^{-1} h^{-1}	740	(Tahir, 2019)
Sodium acetate	V	H_2	Pt	P-type Si nanowires	0.30 mmol L^{-1} h^{-1}	680	(Wan et al., 2015)
COD	V	H_2	Pt	rutile TiO_2	0.07 mmol L^{-1} h^{-1}	13000	(Wang et al., 2013)
COD	I	H_2	Carbon fiber brushes	Si-MoS_x	1.40 mmol L^{-1} h^{-1}	2.30×10^{-6}	(Lu et al., 2019)
Levofloxacin	I	H_2	Graphite rod	Co-N@MoS_2/C	1.86×10^{-3} mmol L^{-1} h^{-1}	60000	(Zeng et al., 2020)
CO_2	III	Acetate	Si/TiO_2	Pt wire	1.2 g L^{-1} d^{-1}	3000	(Liu et al., 2015a)
CO_2	II	Formate	FeOOH/$BiVO_4$	3D TiN-ClFDH	0.02 g L^{-1} d^{-1}	1500	(Kuk et al., 2019)
CO_2	IV (3.0 V)	Isopropanol	CoPi	NiMoZn/stainless-steel	0.04 g L^{-1} d^{-1}	75000	(Torella et al., 2015)
CO_2	IV	Lipid	Carbon brush	Carbon cloth	0.23 g L^{-1} d^{-1}	441.75	(Li et al., 2019)
CO_2	II	Methane	n-TiO_2/FTO	P-InP/Pt	2.45×10^{-6} g L^{-1} d^{-1}	766.67	(Nichols et al., 2015)
HCO_3^-	III	Acetate	Carbon rods	WO_3/MoO_3/g-C_3N_4	0.15 g L^{-1} d^{-1}	2800	(Huang et al., 2021)
HCO_3^-	III	Acetate	Carbon rod	WO_3/MoO_3/g-C_3N_4	0.18 g L^{-1} d^{-1}	2500	(Cai et al., 2020)

Notes: a. Calculation based on the reactor volume with available data; b. Calculation based on the electrode area with available data.

5. Conclusions and future perspectives

This review at first gave a brief introduction to the ins and outs of photo-assisted MESs for synchronous wastewater treatment and bioenergy recovery. Then, on the basis of the systematic bibliometric survey, we summarized and critically assessed the representative achievements and recent advancements of distinct varieties of photo-assisted MESs, from the fundamental mechanism, functional enhancement, and practical application perspectives. First, we systematically classified existing photo-assisted MESs into four main categories, such as bioanode-photocathode MESs, photoanode-biocathode MESs, photomicrobial electrode MESs, as well as photosynthetic bacteria/algae MESs. The corresponding functions performed by semiconductor photoelectrodes and microorganisms in different photo-assisted MESs were also untangled. The semiconductor-microbial MESs (i.e., Type I - III photo-assisted MESs) received more attention than others as they benefited from various electrode modifications with nanotechnology progressed. And the photosynthetic bacteria/algae MESs as a combination of MES technology and algal cultivation, serve as an environmentally friendly platform for recovering bioenergy. Second, we comprehensively dissected and compared current advances of photo-assisted MESs in removing organic and inorganic pollutants and recovering bioenergy (such as electricity, H_2, and other value-added chemicals). In addition, the pollutant removal rate, hydrogen production rate, organic yield, and current density of different systems have also been compared and analyzed. The architecture, anode/cathode materials, ion exchange membrane, and solution chemistry of photo-assisted MESs all show a significant impact on the development of photo-assisted MES technology. Finally, prominent achievements in the field of photo-assisted MESs technology were discussed, as well as present challenges, such as electrode materials optimization, screening and culture of functional microorganisms, large-

559 scale engineering applications of photo-assisted MESs, and future possibilities.

560 Researchers initially utilized non-electrogenic bacteria that required mediators, which
561 restricted MESs application. In the 1990s, the discovery of electrogenic microorganisms like
562 *Shewanella oneidensis* MR-1 and *Geobacter metallireducens* altered the MFCs development
563 by allowing direct electron transmission (Lovley et al., 1993; Venkateswaran et al., 1999).
564 However, MFCs remained notoriously weak electricity generators, thereby prompting the
565 concept of using algae and photosynthetic bacteria to enhance MESs output. Apart from
566 photosynthetic bacteria, semiconductor photoelectrodes have gathered attention due to their
567 excellent photoresponse and electron-hole pairs with reduction/oxidation properties. Therefore,
568 improving the photo-assisted MESs performances can start with the internal structure of the
569 system (electrode materials, microbial species, membrane, etc.,) and operational parameters
570 (temperature, pH, hydraulic retention time, etc.,). In addition, engineering application based on
571 photo-assisted MESs is worth investigating. We offer the following overview and directions
572 related to possible solutions based on diverse challenges faced by current MESs development.

573 **5.1. Optimization of electrode materials**

574 (Bio-)Electrodes as one of the most important components in the construction of photo-
575 assisted MES have always been an essential research item to enhance the entire performance.
576 Activated carbon is one of the most promising non-precious metal materials for oxygen
577 reduction in MFCs since it is low-cost and renewable, which is made from waste biomass. Other
578 carbon-based materials, such as carbon cloth, carbon paper, and carbon fiber, have been widely
579 used as anodes for electroactive biofilms enrichment. However, these carbon-based electrodes
580 usually suffer from inferior EET efficiency and weak microbial affinity. More importantly, the
581 obtained biomass per unit electrode area is too low as the material pores are either too tiny or

too big. Thus, an effective combination of hierarchical pore structures (macro-, meso- and micro-based pores) is necessary (Yi et al., 2020). Yang et al. designed and fabricated a hierarchically structured reduced graphene oxide-polypyrrole (rGO@PPy) nanohybrid as an MES electrode (Yang et al., 2019a). The rGO@PPy electrode could effectively colonize *Geobacter sulfurreducens* and achieve the maximum current density of 4.10 mA cm^{-2}, which is 8-fold higher than that of an rGO electrode. Previous research has demonstrated that the interaction between bioelectrode and photoelectrode determines the conversion efficiency of photo-assisted MESs and the charges produced on both sides of electrodes must match. Thus, the overall efficiency is limited by the comparatively sluggish rate of bioelectrons production. One direction to solving this challenge is to develop conductive 3D electrodes with high surface areas. In addition, building a 3D macroporous interface bioelectrode with good biocompatibility (e.g., polypyrrole and other nitrogen-containing substances) and excellent electrical conductivity (e.g., graphene, metal) could be conducted in parallel to achieve high-efficiency microbial electrocatalysis to improve photo-assisted MESs.

Moreover, the semiconductor photoelectrode, as another electrode material of photo-assisted MESs plays a decisive role in the system performance. Several semiconductor photoelectrodes have been developed to date with outstanding light response performance and favorable stability, such as MoS_3 (Zang et al., 2014), TiO_2 (Du et al., 2014), Cu_2O (Qian et al., 2010), Fe_2O_3 (Zhu et al., 2017). The introduction of semiconductor photoelectrodes renders its possibility to produce value-added chemicals or biofuels without bias. Zeng et al. utilized a photocathode of polydopamine-coated TiO_2 nanotubes for self-sustaining MoS_2 to generate H_2 at a rate of 8.04 mmol L^{-1} h^{-1} without using any external voltage (Zeng et al., 2019). Furthermore, some progress has been achieved in the removal of refractory organics, which bodes well for

605 the future of photo-assisted MESs (Hou et al., 2020). Cost-effectiveness is also another
606 important factor in evaluating the viability of photo-assisted MESs. Thus, it is rejoicing that the
607 photoreactive semiconductor photocathode system can also replace the costly Pt electrode in a
608 bioanode photocathode system (Type I). Overall, it is urgent to explore materials with high-
609 efficiency, strong, scalable, and economical properties to achieve broader photo-assisted MESs
610 application. Carbon-based materials have huge surface areas, good stability, and low cost, but
611 their relatively low electrical conductivity limits their applications. The use of metallic
612 materials as electrodes may increase conductivity, but it comes at a cost. And, it is feasible to
613 increase the catalytic and electrical conductivity of the electrode by doping carbon materials
614 with metal. Furthermore, it is possible to reduce the metal loading by supporting nanomaterials
615 or metal clusters or even single atoms, which can further reduce the cost of investment.

616 **5.2. Screening and culture of functional microorganisms**

617 Microbes metabolize substrates and colonize electrodes to exchange electrons with
618 electrodes, which is critical in the MES process. For example, the bioanodes responsible for
619 metabolizing organic matters are a crucial element in bioanode-photocathode MESs (Type I).
620 The investigation of biocathode as a catalyst in photoanode-biocathode MESs (Type II) is quite
621 fascinating. Research into microbial metabolic pathways in MESs would undoubtedly improve
622 understanding and mastering the role of microorganisms in the system. However, the full
623 potential of these electrochemically active microorganisms (EAMs) has yet to be exploited. In
624 particular, the contradiction between increasing biomass density and lowering mass and
625 electron transport resistance is a major concern. In fact, the internal resistance is frequently
626 exacerbated by poor biofilm conductivity. Therefore, creating an active, conductive, and
627 permeable biofilm will be a key future goal for electrode microbe manipulation. This

necessitates an in-depth knowledge of electrode microorganisms and their EET behavior at the molecular level, as well as microbial genetic engineering and microbial community levels.

Further understanding of molecular mechanisms of the microbe-electrode interaction in photo-assisted MESs remains to be achieved. To date, even the most well-studied EAMs, such as *Geobacter* and *Shewanella*, have yet to be fully recognized in terms of their EET processes. The following four potential pathways are thought to be used by EAMs to donate electrons and/or receive electrons from the solid electrode: (a) cytochrome, which binds to plasma and cell membranes; (b) conductive nanowires; (c) redox mediators; or (d) metabolic intermediates. Furthermore, it has been found that networks of nanowires, cytochrome, and/or specific conducting proteins in the extracellular polymer matrix may be involved in distant electron transfer via extracellular and intercellular electrode communication. This feature is particularly essential for the construction of conductive thick biofilms. Given the variety of EAMs in the natural environment and the possibility of electron transfer among species, more research into EET mechanisms of unknown EAMs species other than *Geobacter* and *Shewanella* is required. It is also worth noting that the EET mechanism of the microbial cathode is much less understood than that of anode biofilms. Although many of the EET routes identified so far at the cathode are identical to those discovered at the anode, the involved microbes and their activities appear to be distinct. Electrotrophic microbial denitrifying bacteria, for example, may take electrons into cells directly or indirectly. Cheng et al. first time revealed that bacteria may directly utilize the electrons generated in the photoelectric chemical process for denitrification using the PEDeN system (biocathode for denitrification combined with TiO_2 photoanode) (Cheng et al., 2017). However, it's unknown exactly how cathode-respiring bacteria get their energy via electron absorption. Extensive improvements in detection techniques will be required for more

efficient, precise, and even in-situ analysis of complicated microbial-electrode interactions.

In the meanwhile, molecular dynamics modeling toolboxes and genetic engineering approaches may aid in the molecular discovery of the EET route. The efficiency of electron transfer can be improved by overexpressing specific proteins of microorganisms through genetic engineering. Zhu et al. increased the bioelectrons supply of *Shewanella oneidensis* by gene modification and overexpression of D-lactate transporter gene SO15222 (Zhu et al., 2017). The results showed that the recombinant *S. oneidensis* (T-SO1522) could digest D-lactate 61% faster than the wild-type *Shewanella oneidensis*. Under illumination, the wild-type *Shewanella oneidensis* and recombinant *Shewanella oneidensis* could achieve the photocurrent with 70 and 95 μA cm^{-2} at 0.8 V vs. Ag/AgCl, respectively, while the abiotic control only generated 16 μA cm^{-2}. From the standpoint of genetic engineering, this is likely to disclose more about the EET mechanism.

To sustain effective, robust biofilm electrodes for practical wastewater treatment, it is also important to maintain a dynamic-balanced microbial population consisting of EAMs and their numerous co-breeding partners and competitors. Of note, some efforts have been on the way to benefit from functional microbes, such as optimizing operating conditions (e.g., pH, temperature, solution properties), creating artificial biological membranes, selective enrichment of microorganisms through electrode surface modification, or using quorum-sensing signal control of the microbial community. In addition, biofilm characteristics including thickness, porosity, conductivity, composition, and extracellular polymeric substance content can significantly affect mass diffusion and electron transfer and thus are also critical for microbial control. More work is still needed in the actual cases.

5.3. Engineering applications of photo-assisted MESs on a large scale

Many variables should be considered in future reactor design based on the feasibility study of prior practical examples. First, regardless of the reactor specifications, a defined distance must be maintained between the anode and cathode to allow for efficient ion transport and lower internal resistance. Longer electrode distances and pH gradients in large-scale systems typically induce this due to increased internal resistance. Shortening the electrode distance, especially in membrane-less photo-assisted MESs, increases the likelihood of oxygen reaching the cathode and the substrate reaching the anode. To produce a sandwiched baffle electrode assembly, a sufficient buffer between two tightly unfolded electrodes is necessary, which may be accomplished in either tubular or plate photo-assisted MESs.

Exploring various hybrid technical combinations is another feasible option to further enhance the practical application of photo-assisted MESs. For example, forward osmosis membranes can be used with a variety of bioreactors, including photo-assisted MESs. Wastewater is typically characterized by low conductivity. By combining photo-assisted MESs with reverse electrodialysis, the wastewater salinity increases during forward osmosis membrane treatment due to increased solution conductivity, thus, reducing the internal resistance of the anode and boosting current density (Logan and Elimelech, 2012). The solution resistance in the cathode chamber can be eliminated by placing the cathode in the absorption solution. Liang et al. successfully modified the battery anode with nano-structured a-Fe_2O_3 (Liang et al., 2016b). Combining with reverse electrodialysis technology, the reactor was designed with three chambers through an anion and cation exchange membrane. At an initial salt concentration of 20 g L^{-1}, the maximum current density of the photo-microbial desalination cell was 8.8 A m^{-2}, which was twice that of the unmodified microbial desalination cell. The effluent of salt concentration in the middle chamber was below 1.4 mg L^{-1}, and the desalination

performance of photo-microbial desalination cells was always higher than 96%. In summary, current photo-microbial desalination cells effectively provide both power generation and desalination (Barahoei et al., 2021).

Mathematical models facilitate better understanding and optimization of such complex hybrid processes. Specifically, two directions may be taken: To begin, a more comprehensive MES model should be developed by factoring in multiple biochemical, hydrodynamic, and electrochemical variables. Second, a global model must explain the entire process, which is centered on photo-assisted MESs, and reflect a variety of sustainability criteria. Photo-assisted MESs may be integrated into mature activated sludge and anaerobic digestion models for unified process simulation, as well as multi-factorial analysis based on mixed process life cycle assessment, to achieve these aims. However, photo-assisted MESs have yet to be adequately proven on a reasonable scale, and sufficient information for such the study is not currently available, life cycle assessment analysis should be undertaken with caution.

Online monitoring and real-time process management are essential to maintain a robust and reliable running. Electrochemical characteristics such as current density and electrode potential may be utilized as important indicators of system status and ongoing-treat level, and provide an effective method of process control, therefore photo-assisted MES is intrinsically capable of real-time monitoring and control. This is somewhat uncharted but promising territory for advancing photo-assisted MESs applications. To this end, more monitoring/control factors, as well as a deeper and more comprehensive understanding of the intricate relationship among engineering, microbiology, and electrochemistry in photo-assisted MESs are required (not just electrochemical parameters, but also traditional biological indicators, water quality parameters, and other basic parameters). Such direct monitoring of biofilm evolution and mass transfer

activities can offer more direct and less intrusive information about the state of the system.

While the technological viability is being further investigated, as well as the economic feasibility and assessment elements are being thoroughly investigated, particularly for photo-assisted MESs that are getting closer to being deployed in actual applications (Yang et al., 2022b). One of the most important economic issues in the scale-up and commercialization of photo-assisted MESs is capital expenses. Therefore, the major goal of current research has frequently been highlighted as the decrease of material and construction costs (Luo et al., 2020). Another direction to the economic assessment can follow to the membrane (separators), usually using ion exchange membranes, which are another costly component of photo-assisted MESs. Searching for low-cost and anti-fouling membrane substitutes (such as non-woven fabrics, ultrafiltration membranes, and forward osmosis membranes) might be a viable approach to reduce costs. However, developing membranes with cheap cost, strong mechanical strength, effective proton transfer, and long-term stability of large-scale systems remains a major issue. To achieve the aim of cost reduction, it is feasible to minimize the usage of ion exchange membranes by developing more single-chamber systems (without membranes) and membrane-electrode-coupled systems (e.g., hollow fiber membrane electrodes).

In conclusion, Photo-assisted MESs, which integrate conventional MESs with semiconductor electrodes, solar cells, photochemical cells, or photosynthetic bacteria, provide preferable techno-economic feasibility for simultaneous wastewater treatment and bioenergy recovery. Nevertheless, to our best knowledge, the studies about photo-assisted MESs are still limited, especially large-scale applications that are at the outset stage. The inevitable challenge of combining the actual day-night intermittent nature of solar light in the field application must be deeply examined. To innovate more efficient, stable, and sustainable photo-assisted MESs

and better adapt and implement them to water/wastewater treatment, more rigid efforts in the reactor scale-up, integration with existing treatment processes, long-term operation, as well as separation and storage of products should be pursued.

CRediT authorship contribution statement

Genping Yi and **Bo Wang**: Conceptualization, Data curation, Writing - original draft. **Yufa Feng** and **Difan Fang**: Formal analysis, Writing - original draft. **Liming Yang**: Conceptualization, Writing - review & editing. **Wenzong Liu** and **Yifeng Zhang**: Formal analysis. **Penghui Shao**: Conceptualization, Data curation. **Spyros G. Pavlostathis**: Conceptualization, Writing - original draft. **Shenglian Luo**, **Xubiao Luo** and **Aijie Wang**: Conceptualization, Writing - review & editing.

Declaration of Competing Interest

The authors declare that they have no known competing financial interests or personal relationships that could have appeared to influence the work reported in this paper.

Acknowledgements

This study was financially supported by the National Science Foundation of China (No. 52060018), the National Science Fund for Distinguished Young Scholars (No. 52125002), the National Key Research and Development Program of China (No. 2019YFC1907900), the Key Project of Research and Development Plan of Jiangxi Province (No. 20201BBE51007), and the Fostering Project of National Science and Technology Awards of Jiangxi Province (No. 20192AEI91001).

References

Ahmadpour, T., Aber, S., Hosseini, M.G., 2020. Improved dye degradation and simultaneous electricity generation in a photoelectrocatalytic microbial fuel cell equipped with AgBr/CuO hybrid photocathode. J. Power Sources 474, 228589. https://doi.org/10.1016/j.jpowsour.2020.228589.

Ali Ansari, S., Mansoob Khan, M., Omaish Ansari, M., Hwan Cho, M., 2015. Improved electrode performance in microbial fuel cells and the enhanced visible light-induced photoelectrochemical behaviour of PtO_x@M-TiO_2 nanocomposites. Ceram. Int. 41 (7), 9131-9139. https://doi.org/10.1016/j.ceramint.2015.03.321.

Arana, T.J., Gude, V.G., 2018. A microbial desalination process with microalgae biocathode using sodium bicarbonate as an inorganic carbon source. Int. Biodeter. Biodegr. 130, 91-97. https://doi.org/10.1016/j.ibiod.2018.04.003.

Barahoei, M., Hatamipour, M.S., Khosravi, M., Afsharzadeh, S., Feghhipour, S.E., 2021. Salinity reduction of brackish water using a chemical photosynthesis desalination cell. Sci. Total Environ. 779, 146473. https://doi.org/10.1016/j.scitotenv.2021.146473.

Bejjanki, D., Muthukumar, K., Radhakrishnan, T.K., Alagarsamy, A., Pugazhendhi, A., Naina Mohamed, S., 2021. Simultaneous bioelectricity generation and water desalination using *Oscillatoria* sp. as biocatalyst in photosynthetic microbial desalination cell. Sci. Total Environ. 754, 142215. https://doi.org/10.1016/j.scitotenv.2020.142215.

Bennani, Y., Peters, M.C.F.M., Appel, P.W., Rietveld, L.C., 2015. Electrochemically active biofilm and photoelectrocatalytic regeneration of the titanium dioxide composite electrode for advanced oxidation in water treatment. Electrochim. Acta 182, 604-612. https://doi.org/10.1016/j.electacta.2015.09.101.

Brune, A., Jeong, G., Liddell, P.A., Sotomura, T., Moore, T.A., Moore, A.L., Gust, D., 2004. Porphyrin-sensitized nanoparticulate TiO_2 as the photoanode of a hybrid photoelectrochemical biofuel cell. Langmuir 20 (19), 8366-8371. https://doi.org/10.1021/la048974i.

Cai, Z., Huang, L., Quan, X., Zhao, Z., Shi, Y., Li Puma, G., 2020. Acetate production from inorganic carbon (HCO_3^-) in photo-assisted biocathode microbial electrosynthesis systems using WO_3/MoO_3/g-C_3N_4 heterojunctions and *Serratia marcescens* species. Appl. Catal. B-Environ. 267, 118611. https://doi.org/10.1016/j.apcatb.2020.118611.

Cao, X., Huang, X., Boon, N., Liang, P., Fan, M., 2008. Electricity generation by an enriched phototrophic consortium in a microbial fuel cell. Electrochem. Commun. 10 (9), 1392-1395. https://doi.org/10.1016/j.elecom.2008.07.008.

Cao, X., Huang, X., Liang, P., Boon, N., Fan, M., Zhang, L., Zhang, X., 2009. A completely anoxic microbial fuel cell using a photo-biocathode for cathodic carbon dioxide reduction. Energ. Environ. Sci. 2 (5), 498-501. https://doi.org/10.1039/B901069F.

Chae, K.-J., Choi, M.-J., Kim, K.-Y., Ajayi, F.F., Chang, I.-S., Kim, I.S., 2009. A solar-powered microbial electrolysis cell with a platinum catalyst-free cathode to produce hydrogen. Environ. Sci. Technol. 43 (24), 9525-9530. https://doi.org/10.1021/es9022317.

Chen, Q.-Y., Liu, J.-S., Liu, Y., Wang, Y.-H., 2013a. Hydrogen production on TiO_2 nanorod arrays cathode coupling with bio-anode with additional electricity generation. J. Power Sources 238, 345-349. https://doi.org/10.1016/j.jpowsour.2013.04.066.

Chen, Z., Lyu, Y., Wang, K., Dong, X., Deng, M., Bai, C., Xu, Y., Zhang, W., Liu, Z., 2013b. Preparation of a microalgal photoanode for hydrogen production by photo-

bioelectrochemical water-splitting. Int. J. Hydrogen. Energ. 38 (29), 13045-13049. https://doi.org/10.1016/j.ijhydene.2013.03.095.

Cheng, H.-Y., Tian, X.-D., Li, C.-H., Wang, S.-S., Su, S.-G., Wang, H.-C., Zhang, B., Sharif, H.M.A., Wang, A.-J., 2017. Microbial photoelectrotrophic denitrification as a sustainable and efficient way for reducing nitrate to nitrogen. Environ. Sci. Technol. 51 (21), 12948-12955. https://doi.org/10.1021/acs.est.7b02557.

Cheng, S., Logan, B.E., 2007. Sustainable and efficient biohydrogen production via electrohydrogenesis. P. Natl. Acad. Sci. USA 104 (47), 18871. https://doi.org/10.1073/pnas.0706379104.

Chu, N., Liang, Q., Jiang, Y., Zeng, R.J., 2020. Microbial electrochemical platform for the production of renewable fuels and chemicals. Biosens. Bioelectron. 150, 111922. https://doi.org/10.1016/j.bios.2019.111922.

Colombo, A., Marzorati, S., Lucchini, G., Cristiani, P., Pant, D., Schievano, A., 2017. Assisting cultivation of photosynthetic microorganisms by microbial fuel cells to enhance nutrients recovery from wastewater. Bioresource Technol. 237, 240-248. https://doi.org/10.1016/j.biortech.2017.03.038.

Darus, L., Ledezma, P., Keller, J., Freguia, S., 2014. Oxygen suppresses light-driven anodic current generation by a mixed phototrophic culture. Environ. Sci. Technol. 48 (23), 14000-14006. https://doi.org/10.1021/es5024702.

Darus, L., Lu, Y., Ledezma, P., Keller, J., Freguia, S., 2015. Fully reversible current driven by a dual marine photosynthetic microbial community. Bioresource Technol. 195, 248-253. https://doi.org/10.1016/j.biortech.2015.06.055.

Ding, H., Li, Y., Lu, A., Jin, S., Quan, C., Wang, C., Wang, X., Zeng, C., Yan, Y., 2010. Photocatalytically improved azo dye reduction in a microbial fuel cell with rutile-cathode. Bioresource Technol. 101 (10), 3500-3505. https://doi.org/10.1016/j.biortech.2009.11.107.

Du, Y., Feng, Y., Qu, Y., Liu, J., Ren, N., Liu, H., 2014. Electricity generation and pollutant degradation using a novel biocathode coupled photoelectrochemical cell. Environ. Sci. Technol. 48 (13), 7634-7641. https://doi.org/10.1021/es5011994.

Efrati, A., Lu, C.-H., Michaeli, D., Nechushtai, R., Alsaoub, S., Schuhmann, W., Willner, I., 2016. Assembly of photo-bioelectrochemical cells using photosystem I-functionalized electrodes. Nat. Energy 1 (2), 15021. https://doi.org/10.1038/nenergy.2015.21.

Feng, H., Liang, Y., Guo, K., Li, N., Shen, D., Cong, Y., Zhou, Y., Wang, Y., Wang, M., Long, Y., 2016. Hybridization of photoanode and bioanode to enhance the current production of bioelectrochemical systems. Water Res. 102, 428-435. https://doi.org/10.1016/j.watres.2016.06.061.

Feng, H., Tang, C., Wang, Q., Liang, Y., Shen, D., Guo, K., He, Q., Jayaprada, T., Zhou, Y., Chen, T., Ying, X., Wang, M., 2018. A novel photoactive and three-dimensional stainless steel anode dramatically enhances the current density of bioelectrochemical systems. Chemosphere 196, 476-481. https://doi.org/10.1016/j.chemosphere.2017.12.166.

Fischer, F., 2018. Photoelectrode, photovoltaic and photosynthetic microbial fuel cells. Renew. Sust. Energ. Rev. 90, 16-27. https://doi.org/10.1016/j.rser.2018.03.053.

Guo, D., Song, R.-B., Shao, H.-H., Zhang, J.-R., Zhu, J.-J., 2017. Visible-light-enhanced power generation in microbial fuel cells coupling with 3D nitrogen-doped graphene. Chem. Commun. 53 (72), 9967-9970. https://doi.org/10.1039/C7CC04666A.

Guo, D., Wei, H.-F., Yu, X.-Y., Xia, Q., Chen, Z., Zhang, J.-R., Song, R.-B., Zhu, J.-J., 2019.

Plasmon-enhanced cathodic reduction for accelerating electricity generation in visible-light-assisted microbial fuel cells. Nano Energy 57, 94-100. https://doi.org/10.1016/j.nanoen.2018.12.043.

Han, H.-X., Shi, C., Yuan, L., Sheng, G.-P., 2017. Enhancement of methyl orange degradation and power generation in a photoelectrocatalytic microbial fuel cell. Appl. Energ. 204, 382-389. https://doi.org/10.1016/j.apenergy.2017.07.032.

Han, L., Bai, L., Zhu, C., Wang, Y., Dong, S., 2012. Improving the performance of a membraneless and mediatorless glucose-air biofuel cell with a TiO_2 nanotube photoanode. Chem. Commun. 48 (49), 6103-6105. https://doi.org/10.1039/C2CC32168H.

He, H., Zhou, M., Yang, J., Hu, Y., Zhao, Y., 2014. Simultaneous wastewater treatment, electricity generation and biomass production by an immobilized photosynthetic algal microbial fuel cell. Bioproc. Biosyst. Eng. 37 (5), 873-880. https://doi.org/10.1007/s00449-013-1058-4.

He, Z., Kan, J., Mansfeld, F., Angenent, L.T., Nealson, K.H., 2009. Self-sustained phototrophic microbial fuel cells based on the synergistic cooperation between photosynthetic microorganisms and heterotrophic bacteria. Environ. Sci. Technol. 43 (5), 1648-1654. https://doi.org/10.1021/es803084a.

Hou, Y., Gan, Y., Yu, Z., Chen, X., Qian, L., Zhang, B., Huang, L., Huang, J., 2017a. Solar promoted azo dye degradation and energy production in the bio-photoelectrochemical system with a g-C_3N_4/BiOBr heterojunction photocathode. J. Power Sources 371, 26-34. https://doi.org/10.1016/j.jpowsour.2017.10.033.

Hou, Y., Yuan, G., Qin, S., Tu, L., Yan, Y., Yu, Z., Lin, H., Chen, Y., Zhu, H., Song, H., Wang, S., 2020. Photocathode optimization and microbial community in the solar-illuminated bio-photoelectrochemical system for nitrofurazone degradation. Bioresource Technol. 302, 122761. https://doi.org/10.1016/j.biortech.2020.122761.

Hou, Y., Zhang, R., Yu, Z., Huang, L., Liu, Y., Zhou, Z., 2017b. Accelerated azo dye degradation and concurrent hydrogen production in the single-chamber photocatalytic microbial electrolysis cell. Bioresource Technol. 224, 63-68. https://doi.org/10.1016/j.biortech.2016.10.069.

Huang, L., Song, S., Cai, Z., Zhou, P., Li Puma, G., 2021. Efficient conversion of bicarbonate (HCO_3^-) to acetate and simultaneous heavy metal Cr(VI) removal in photo-assisted microbial electrosynthesis systems combining WO_3/MoO_3/g-C_3N_4 heterojunctions and Serratia marcescens electrotroph. Chem. Eng. J. 406, 126786. https://doi.org/10.1016/j.cej.2020.126786.

Jeon, Y., Kim, J.H., Koo, K., Kim, S., 2018. A photo-assisted microbial electrolysis cell for the exclusive biohydrogen production using a MoS_2-coated p-type copper oxide. J. Power Sources 373, 79-84. https://doi.org/10.1016/j.jpowsour.2017.11.003.

Kokabian, B., Ghimire, U., Gude, V.G., 2018a. Water deionization with renewable energy production in microalgae-microbial desalination process. Renew. Energ. 122, 354-361. https://doi.org/10.1016/j.renene.2018.01.061.

Kokabian, B., Gude, V.G., 2015. Sustainable photosynthetic biocathode in microbial desalination cells. Chem. Eng. J. 262, 958-965. https://doi.org/10.1016/j.cej.2014.10.048.

Kokabian, B., Smith, R., Brooks, J.P., Gude, V.G., 2018b. Bioelectricity production in photosynthetic microbial desalination cells under different flow configurations. J. Ind. Eng. Chem. 58, 131-139. https://doi.org/10.1016/j.jiec.2017.09.017.

Kong, F., Ren, H.-Y., Pavlostathis, S.G., Nan, J., Ren, N.-Q., Wang, A., 2020. Overview of value-added products bioelectrosynthesized from waste materials in microbial electrosynthesis systems. Renew. Sust. Energ. Rev. 125, 109816. https://doi.org/10.1016/j.rser.2020.109816.

Kuk, S.K., Ham, Y., Gopinath, K., Boonmongkolras, P., Lee, Y., Lee, Y.W., Kondaveeti, S., Ahn, C., Shin, B., Lee, J.-K., Jeon, S., Park, C.B., 2019. Continuous 3D titanium nitride nanoshell structure for solar-driven unbiased biocatalytic CO_2 reduction. Adv. Energy Mater. 9 (25), 1900029. https://doi.org/10.1002/aenm.201900029.

Lai, Y.-C., Liang, C.-M., Hsu, S.-C., Hsieh, P.-H., Hung, C.-H., 2017. Polyphosphate metabolism by purple non-sulfur bacteria and its possible application on photo-microbial fuel cell. J. Biosci. Bioeng. 123 (6), 722-730. https://doi.org/10.1016/j.jbiosc.2017.01.012.

Lam, S.-M., Sin, J.-C., Zeng, H., Lin, H., Li, H., Mohamed, A.R., Lim, J.W., 2022. Ameliorating Cu^{2+} reduction in microbial fuel cell with Z-scheme $BiFeO_3$ decorated on flower-like ZnO composite photocathode. Chemosphere 287, 132384. https://doi.org/10.1016/j.chemosphere.2021.132384.

Li, D.-B., Cheng, Y.-Y., Li, L.-L., Li, W.-W., Huang, Y.-X., Pei, D.-N., Tong, Z.-H., Mu, Y., Yu, H.-Q., 2014a. Light-driven microbial dissimilatory electron transfer to hematite. Phys. Chem. Chem. Phys. 16 (42), 23003-23011. https://doi.org/10.1039/C4CP04065A.

Li, G., Feng, X., Fei, J., Cai, P., Li, J., Huang, J., Li, J., 2017. Interfacial assembly of photosystem II with conducting polymer films toward enhanced photo-bioelectrochemical cells. Adv. Mater. Interfaces 4 (1), 1600619. https://doi.org/10.1002/admi.201600619.

Li, J., Feng, X., Fei, J., Cai, P., Huang, J., Li, J., 2016a. Integrating photosystem II into a porous TiO_2 nanotube network toward highly efficient photo-bioelectrochemical cells. J. Mater. Chem. A 4 (31), 12197-12204. https://doi.org/10.1039/C6TA04964H.

Li, M., Zhou, M., Tan, C., Tian, X., 2019. Enhancement of CO_2 biofixation and bioenergy generation using a novel airlift type photosynthetic microbial fuel cell. Bioresource Technol. 272, 501-509. https://doi.org/10.1016/j.biortech.2018.10.078.

Li, W.-W., Yu, H.-Q., He, Z., 2014b. Towards sustainable wastewater treatment by using microbial fuel cells-centered technologies. Energ. Environ. Sci. 7 (3), 911-924. https://doi.org/10.1039/C3EE43106A.

Li, Y., Lu, A., Ding, H., Jin, S., Yan, Y., Wang, C., Zen, C., Wang, X., 2009. Cr(VI) reduction at rutile-catalyzed cathode in microbial fuel cells. Electrochem. Commun. 11 (7), 1496-1499. https://doi.org/10.1016/j.elecom.2009.05.039.

Li, Y., Yang, H.-Y., Shen, J.-Y., Mu, Y., Yu, H.-Q., 2016b. Enhancement of azo dye decolourization in a MFC-MEC coupled system. Bioresource Technol. 202, 93-100. https://doi.org/10.1016/j.biortech.2015.11.079.

Liang, D., Han, G., Zhang, Y., Rao, S., Lu, S., Wang, H., Xiang, Y., 2016a. Efficient H_2 production in a microbial photoelectrochemical cell with a composite Cu_2O/NiO_x photocathode under visible light. Appl. Energ. 168, 544-549. https://doi.org/10.1016/j.apenergy.2016.01.118.

Liang, Y., Feng, H., Shen, D., Li, N., Long, Y., Zhou, Y., Gu, Y., Ying, X., Dai, Q., 2016b. A high-performance photo-microbial desalination cell. Electrochim. Acta 202, 197-202. https://doi.org/10.1016/j.electacta.2016.03.177.

Liang, Y., Feng, H., Shen, D., Long, Y., Li, N., Zhou, Y., Ying, X., Gu, Y., Wang, Y., 2016c. Metal-based anode for high performance bioelectrochemical systems through photo-

electrochemical interaction. J. Power Sources 324, 26-32. https://doi.org/10.1016/j.jpowsour.2016.05.059.

Lin, Z.-Q., Yuan, S.-J., Li, W.-W., Chen, J.-J., Sheng, G.-P., Yu, H.-Q., 2017. Denitrification in an integrated bioelectro-photocatalytic system. Water Res. 109, 88-93. https://doi.org/10.1016/j.watres.2016.11.042.

Liu, C., Gallagher, J.J., Sakimoto, K.K., Nichols, E.M., Chang, C.J., Chang, M.C.Y., Yang, P., 2015a. Nanowire-bacteria hybrids for unassisted solar carbon dioxide fixation to value-added chemicals. Nano Lett. 15 (5), 3634-3639. https://doi.org/10.1021/acs.nanolett.5b01254.

Liu, T., Rao, L., Yuan, Y., Zhuang, L., 2015b. Bioelectricity generation in a microbial fuel cell with a self-sustainable photocathode. The Scientific World Journal 2015, 864568. https://doi.org/10.1155/2015/864568.

Liu, W., Lin, L., Qie, Y., Meng, Y., Luan, F., 2022. Continuous and efficient uranium recovery in a bioelectrochemical system. Resour. Conserv. Recy. 177, 105993. https://doi.org/10.1016/j.resconrec.2021.105993.

Logan, B.E., Elimelech, M., 2012. Membrane-based processes for sustainable power generation using water. Nature 488 (7411), 313-319. https://doi.org/10.1038/nature11477.

Logan, B.E., Hamelers, B., Rozendal, R., Schröder, U., Keller, J., Freguia, S., Aelterman, P., Verstraete, W., Rabaey, K., 2006. Microbial fuel cells: Methodology and technology. Environ. Sci. Technol. 40 (17), 5181-5192. https://doi.org/10.1021/es0605016.

Logan, B.E., Rabaey, K., 2012. Conversion of wastes into bioelectricity and chemicals by using microbial electrochemical technologies. Science 337 (6095), 686. https://doi.org/10.1126/science.1217412.

Long, X., Wang, H., Wang, C., Cao, X., Li, X., 2019. Enhancement of azo dye degradation and power generation in a photoelectrocatalytic microbial fuel cell by simple cathodic reduction on titania nanotube arrays electrode. J. Power Sources 415, 145-153. https://doi.org/10.1016/j.jpowsour.2019.01.069.

Lovley, D.R., Giovannoni, S.J., White, D.C., Champine, J.E., Phillips, E.J.P., Gorby, Y.A., Goodwin, S., 1993. *Geobacter metallireducens* gen. nov. sp. nov., a microorganism capable of coupling the complete oxidation of organic compounds to the reduction of iron and other metals. Arch. Microbiol. 159 (4), 336-344. 10.1007/BF00290916.

Lu, A., Li, Y., 2012. Light fuel cell (LFC): A novel device for interpretation of microorganisms-involved mineral photochemical process. Geomicrobiol. J. 29 (3), 236-243. https://doi.org/10.1080/01490451.2011.575911.

Lu, A., Li, Y., Jin, S., Ding, H., Zeng, C., Wang, X., Wang, C., 2010. Microbial fuel cell equipped with a photocatalytic rutile-coated cathode. Energ. Fuel. 24 (2), 1184-1190. https://doi.org/10.1021/ef901053j.

Lu, L., Vakki, W., Aguiar, J.A., Xiao, C., Hurst, K., Fairchild, M., Chen, X., Yang, F., Gu, J., Ren, Z.J., 2019. Unbiased solar H_2 production with current density up to 23 mA cm^{-2} by Swiss-cheese black Si coupled with wastewater bioanode. Energ. Environ. Sci. 12 (3), 1088-1099. https://doi.org/10.1039/C8EE03673J.

Lu, L., Williams, N.B., Turner, J.A., Maness, P.-C., Gu, J., Ren, Z.J., 2017. Microbial photoelectrosynthesis for self-sustaining hydrogen generation. Environ. Sci. Technol. 51 (22), 13494-13501. https://doi.org/10.1021/acs.est.7b03644.

Luo, S., Sai Shankar Sampara, P., He, Z., 2018. Effective algal harvesting by using mesh

membrane for enhanced energy recovery in an innovative integrated photobioelectrochemical system. Bioresource Technol. 253, 33-40. https://doi.org/10.1016/j.biortech.2018.01.001.

Luo, S., Waller, L., Badgley, B., He, Z., Young, E.B., 2020. Effects of bacterial inoculation and nitrogen loading on bacterial-algal consortium composition and functions in an integrated photobioelectrochemical system. Sci. Total Environ. 716, 137135. https://doi.org/10.1016/j.scitotenv.2020.137135.

Mateo, S., Gonzalez del Campo, A., Cañizares, P., Lobato, J., Rodrigo, M.A., Fernandez, F.J., 2014. Bioelectricity generation in a self-sustainable microbial solar cell. Bioresource Technol. 159, 451-454. https://doi.org/10.1016/j.biortech.2014.03.059.

McCormick, A.J., Bombelli, P., Bradley, R.W., Thorne, R., Wenzel, T., Howe, C.J., 2015. Biophotovoltaics: oxygenic photosynthetic organisms in the world of bioelectrochemical systems. Energ. Environ. Sci. 8 (4), 1092-1109. https://doi.org/10.1039/C4EE03875D.

Mu, Y., Rabaey, K., Rozendal, R.A., Yuan, Z., Keller, J., 2009. Decolorization of azo dyes in bioelectrochemical systems. Environ. Sci. Technol. 43 (13), 5137-5143. https://doi.org/10.1021/es900057f.

Naina Mohamed, S., Jayabalan, T., Muthukumar, K., 2019. Simultaneous bioenergy generation and carbon dioxide sequestration from food wastewater using algae microbial fuel cell. Energ. Source. Part A, 1-9. https://doi.org/10.1080/15567036.2019.1666932.

Nakamura, R., Kai, F., Okamoto, A., Newton, G.J., Hashimoto, K., 2009. Self-constructed electrically conductive bacterial networks. Angew. Chem. 48 (3), 508-511. https://doi.org/10.1002/ange.200804750.

Nichols, E.M., Gallagher, J.J., Liu, C., Su, Y., Resasco, J., Yu, Y., Sun, Y., Yang, P., Chang, M.C.Y., Chang, C.J., 2015. Hybrid bioinorganic approach to solar-to-chemical conversion. P. Natl. Acad. Sci. USA 112 (37), 11461. https://doi.org/10.1073/pnas.1508075112.

Pan, M., Su, Y., Zhu, X., Pan, G., Zhang, Y., Angelidaki, I., 2021. Bioelectrochemically assisted sustainable conversion of industrial organic wastewater and clean production of microalgal protein. Resour. Conserv. Recy. 168, 105441. https://doi.org/10.1016/j.resconrec.2021.105441.

Qi, X., Bo, Y., Ren, Y., Wang, X., 2018. The anaerobic biodegradation of poly(lactic) acid textiles in photosynthetic microbial fuel cells: Self-sustained bioelectricity generation. Polym. Degrad. Stabil. 148, 42-49. https://doi.org/10.1016/j.polymdegradstab.2018.01.005.

Qian, F., Wang, G., Li, Y., 2010. Solar-driven microbial photoelectrochemical cells with a nanowire photocathode. Nano Lett. 10 (11), 4686-4691. https://doi.org/10.1021/nl102977n.

Qian, F., Wang, H., Ling, Y., Wang, G., Thelen, M.P., Li, Y., 2014. Photoenhanced electrochemical interaction between *Shewanella* and a hematite nanowire photoanode. Nano Lett. 14 (6), 3688-3693. https://doi.org/10.1021/nl501664n.

Qin, S., Hou, Y., Yuan, G., Yu, Z., Tu, L., Yan, Y., Chen, S., Sun, J., Lan, D., Wang, S., 2020. Different refractory organic substances degradation and microbial community shift in the single-chamber bio-photoelectrochemical system. Bioresource Technol. 307, 123176. https://doi.org/10.1016/j.biortech.2020.123176.

Ren, G., Sun, Y., Lu, A., Li, Y., Ding, H., 2018. Boosting electricity generation and Cr(VI) reduction based on a novel silicon solar cell coupled double-anode (photoanode/bioanode)

microbial fuel cell. J. Power Sources 408, 46-50. https://doi.org/10.1016/j.jpowsour.2018.10.081.

Riedel, M., Wersig, J., Ruff, A., Schuhmann, W., Zouni, A., Lisdat, F., 2019. A Z-scheme-inspired photobioelectrochemical H_2O/O_2 Cell with a 1 V open-circuit voltage combining photosystem II and PbS quantum dots. Angew. Chem. Int. Edit. 58 (3), 801-805. https://doi.org/10.1002/anie.201811172.

Shan, Y., Cui, J., Liu, Y., Zhao, W., 2020. TiO_2 anchored on MoS_2 nanosheets based on molybdenite exfoliation as an efficient cathode for enhanced Cr(VI) reduction in microbial fuel cell. Environ. Res. 190, 110010. https://doi.org/10.1016/j.envres.2020.110010.

Shi, H., Jiang, X., Chen, D., Li, Y., Hou, C., Wang, L., Shen, J., 2020. $BiVO_4$/FeOOH semiconductor-microbe interface for enhanced visible-light-driven biodegradation of pyridine. Water Res. 187, 116464. https://doi.org/10.1016/j.watres.2020.116464.

Shukla, M., Kumar, S., 2018. Algal growth in photosynthetic algal microbial fuel cell and its subsequent utilization for biofuels. Renew. Sust. Energ. Rev. 82, 402-414. https://doi.org/10.1016/j.rser.2017.09.067.

Slate, A.J., Whitehead, K.A., Brownson, D.A.C., Banks, C.E., 2019. Microbial fuel cells: An overview of current technology. Renew. Sust. Energ. Rev. 101, 60-81. https://doi.org/10.1016/j.rser.2018.09.044.

Strik, D.P.B.T.B., Hamelers, H.V.M., Buisman, C.J.N., 2010. Solar energy powered microbial fuel cell with a reversible bioelectrode. Environ. Sci. Technol. 44 (1), 532-537. https://doi.org/10.1021/es902435v.

Sun, J., Cai, B., Xu, W., Huang, Y., Zhang, Y., Peng, Y., Chang, K., Kuo, J., Chen, K., Ning, X., Liu, G., Wang, Y., Yang, Z., Liu, J., 2017. Enhanced bioelectricity generation and azo dye treatment in a reversible photo-bioelectrochemical cell by using novel anthraquinone-2,6-disulfonate (AQDS)/MnO_x-doped polypyrrole film electrodes. Bioresource Technol. 225, 40-47. https://doi.org/10.1016/j.biortech.2016.11.038.

Sun, J., Liu, L., Yang, F., 2020a. Successful bio-electrochemical treatment of nitrogenous mariculture wastewater by enhancing nitrogen removal via synergy of algae and cathodic photo-electro-catalysis. Sci. Total Environ. 743, 140738. https://doi.org/10.1016/j.scitotenv.2020.140738.

Sun, J., Xu, W., Cai, B., Huang, G., Zhang, H., Zhang, Y., Yuan, Y., Chang, K., Chen, K., Peng, Y., Chen, K., 2019. High-concentration nitrogen removal coupling with bioelectric power generation by a self-sustaining algal-bacterial biocathode photo-bioelectrochemical system under daily light/dark cycle. Chemosphere 222, 797-809. https://doi.org/10.1016/j.chemosphere.2019.01.191.

Sun, J., Yang, P., Li, N., Zhao, M., Zhang, X., Zhang, Y., Yuan, Y., Lu, X., Lu, X., 2020b. Extraction of photosynthetic electron from mixed photosynthetic consortium of bacteria and algae towards sustainable bioelectrical energy harvesting. Electrochim. Acta 336, 135710. https://doi.org/10.1016/j.electacta.2020.135710.

Tahir, M.B., 2019. Microbial photoelectrochemical cell for improved hydrogen evolution using nickel ferrite incorporated WO_3 under visible light irradiation. Int. J. Hydrogen. Energ. 44 (32), 17316-17322. https://doi.org/10.1016/j.ijhydene.2019.01.067.

Thorne, R., Hu, H., Schneider, K., Bombelli, P., Fisher, A., Peter, L.M., Dent, A., Cameron, P.J., 2011. Porous ceramic anode materials for photo-microbial fuel cells. J. Mater. Chem. 21 (44), 18055-18060. https://doi.org/10.1039/C1JM13058G.

Torella, J.P., Gagliardi, C.J., Chen, J.S., Bediako, D.K., Colón, B., Way, J.C., Silver, P.A., Nocera, D.G., 2015. Efficient solar-to-fuels production from a hybrid microbial-water-splitting catalyst system. P. Natl. Acad. Sci. USA 112 (8), 2337. https://doi.org/10.1073/pnas.1424872112.

Venkateswaran, K., Moser, D.P., Dollhopf, M.E., Lies, D.P., Saffarini, D.A., MacGregor, B.J., Ringelberg, D.B., White, D.C., Nishijima, M., Sano, H., Burghardt, J., Stackebrandt, E., Nealson, K.H., 1999. Polyphasic taxonomy of the genus *Shewanella* and description of *Shewanella* oneidensis sp. nov. Int. J. Syst. Bacteriol. 49 (2), 705-724. https://doi.org/10.1099/00207713-49-2-705.

Wan, L.-L., Li, X.-J., Zang, G.-L., Wang, X., Zhang, Y.-Y., Zhou, Q.-X., 2015. A solar assisted microbial electrolysis cell for hydrogen production driven by a microbial fuel cell. RSC Adv. 5 (100), 82276-82281. https://doi.org/10.1039/C5RA16919D.

Wang, B., Liu, W., Zhang, Y., Wang, A., 2020a. Bioenergy recovery from wastewater accelerated by solar power: Intermittent electro-driving regulation and capacitive storage in biomass. Water Res. 175, 115696. https://doi.org/10.1016/j.watres.2020.115696.

Wang, B., Liu, W., Zhang, Y., Wang, A., 2020b. Intermittent electro field regulated mutualistic interspecies electron transfer away from the electrodes for bioenergy recovery from wastewater. Water Res. 185, 116238. https://doi.org/10.1016/j.watres.2020.116238.

Wang, H., Qian, F., Li, Y., 2014a. Solar-assisted microbial fuel cells for bioelectricity and chemical fuel generation. Nano Energy 8, 264-273. https://doi.org/10.1016/j.nanoen.2014.06.004.

Wang, H., Qian, F., Wang, G., Jiao, Y., He, Z., Li, Y., 2013. Self-biased solar-microbial device for sustainable hydrogen generation. ACS Nano 7 (10), 8728-8735. https://doi.org/10.1021/nn403082m.

Wang, H., Ren, Z.J., 2013. A comprehensive review of microbial electrochemical systems as a platform technology. Biotechnol. Adv. 31 (8), 1796-1807. https://doi.org/10.1016/j.biotechadv.2013.10.001.

Wang, L., Liu, L., Yang, F., 2018. Efficient gas phase VOC removal and electricity generation in an integrated bio-photo-electro-catalytic reactor with bio-anode and TiO_2 photo-electro-catalytic air cathode. Bioresource Technol. 270, 554-561. https://doi.org/10.1016/j.biortech.2018.09.041.

Wang, L., Tian, L., Deng, X., Zhang, M., Sun, S., Zhang, W., Zhao, L., Chen, Q.-Y., Liu, J.-S., Liu, Y., Wang, Y.-H., 2014b. Photosensitizers from spirulina for solar cell hydrogen production on TiO_2 nanorod arrays cathode coupling with bio-anode with additional electricity generation. J. Chem.-ny 2014, 430806-430349. https://doi.org/10.1016/j.jpowsour.2013.04.066.

Wang, S., Yang, X., Zhu, Y., Su, Y., Li, C., 2014c. Solar-assisted dual chamber microbial fuel cell with a $CuInS_2$ photocathode. RSC Adv. 4 (45), 23790-23796. https://doi.org/10.1039/C4RA02488E.

Wang, Y., Lin, Z., Su, X., Zhao, P., Zhou, J., He, Q., Ai, H., 2019. Cost-effective domestic wastewater treatment and bioenergy recovery in an immobilized microalgal-based photoautotrophic microbial fuel cell (PMFC). Chem. Eng. J. 372, 956-965. https://doi.org/10.1016/j.cej.2019.05.004.

Weliwatte, N.S., Minteer, S.D., 2021. Photo-bioelectrocatalytic CO_2 reduction for a circular energy landscape. Joule 5 (10), 2564-2592. https://doi.org/10.1016/j.joule.2021.08.003.

Wong, M.T., Cheng, D., Wang, R., Hsing, I.M., 2016. Modifying the endogenous electron fluxes of *Rhodobacter sphaeroides* 2.4.1 for improved electricity generation. Enzyme Microb. Tech. 86, 45-51. https://doi.org/10.1016/j.enzmictec.2016.01.009.

Wu, Y.-c., Wang, Z.-j., Zheng, Y., Xiao, Y., Yang, Z.-h., Zhao, F., 2014. Light intensity affects the performance of photo microbial fuel cells with *Desmodesmus* sp. A8 as cathodic microorganism. Appl. Energ. 116, 86-90. https://doi.org/10.1016/j.apenergy.2013.11.066.

Xiao, L., Young, E.B., Berges, J.A., He, Z., 2012. Integrated photo-bioelectrochemical system for contaminants removal and bioenergy production. Environ. Sci. Technol. 46 (20), 11459-11466. https://doi.org/10.1021/es303144n.

Yang, F., Ke, Z., Li, Z., Patrick, M., Abboud, Z., Yamamoto, N., Xiao, X., Gu, J., 2020. Photo/bio-electrochemical systems for environmental remediation and energy harvesting. ChemSusChem 13 (13), 3391-3403. https://doi.org/10.1002/cssc.202000203.

Yang, L., Yi, G., Hou, Y., Cheng, H., Luo, X., Pavlostathis, S.G., Luo, S., Wang, A., 2019a. Building electrode with three-dimensional macroporous interface from biocompatible polypyrrole and conductive graphene nanosheets to achieve highly efficient microbial electrocatalysis. Biosens. Bioelectron. 141, 111444. https://doi.org/10.1016/j.bios.2019.111444.

Yang, L., Yi, G., Wang, B., Shao, P., Feng, Y., Liu, Y., Yu, K., Liu, F., Liu, L., Luo, X., Luo, S., 2022a. Atomic H* enhanced electrochemical recovery towards high-value-added metallic Sb from complex mine flotation wastewater. Resour. Conserv. Recy. 178, 106020. https://doi.org/10.1016/j.resconrec.2021.106020.

Yang, Q., Bao, X., Li, Z., Yang, A., Cao, Y., Hu, X., Yu, L., Liu, B., 2022b. Visible-light-enhanced Cr(VI) reduction and bioelectricity generation at MXene photocathode in photoelectrocatalytic microbial fuel cells. J. Water Process Eng. 45, 102454. https://doi.org/10.1016/j.jwpe.2021.102454.

Yang, Z., Zhang, L., Nie, C., Hou, Q., Zhang, S., Pei, H., 2019b. Multiple anodic chambers sharing an algal raceway pond to establish a photosynthetic microbial fuel cell stack: Voltage boosting accompany wastewater treatment. Water Res. 164, 114955. https://doi.org/10.1016/j.watres.2019.114955.

Yi, G., Cui, D., Yang, L., Fang, D., Chang, Z., Cheng, H., Shao, P., Luo, X., Wang, A., 2020. Bacteria-affinity aminated carbon nanotubes bridging reduced graphene oxide for highly efficient microbial electrocatalysis. Environ. Res. 191, 110212. https://doi.org/10.1016/j.envres.2020.110212.

Yuan, S.-J., Sheng, G.-P., Li, W.-W., Lin, Z.-Q., Zeng, R.J., Tong, Z.-H., Yu, H.-Q., 2010. Degradation of organic pollutants in a photoelectrocatalytic system enhanced by a microbial fuel cell. Environ. Sci. Technol. 44 (14), 5575-5580. https://doi.org/10.1021/es101317z.

Zang, G.-L., Sheng, G.-P., Shi, C., Wang, Y.-K., Li, W.-W., Yu, H.-Q., 2014. A bio-photoelectrochemical cell with a MoS_3-modified silicon nanowire photocathode for hydrogen and electricity production. Energ. Environ. Sci. 7 (9), 3033-3039. http://dx.doi.org/10.1039/C4EE00654B.

Zeng, L., Li, X., Fan, S., Yin, Z., Mu, J., Qin, M., Chen, A., 2020. Solar-driven bio-electro-chemical system for synergistic hydrogen evolution and pollutant elimination simultaneously over defect-rich CoN-MoS_2/biomass nanosheets. J. Power Sources 478, 228755. https://doi.org/10.1016/j.jpowsour.2020.228755.

Zeng, L., Li, X., Fan, S., Zhang, M., Yin, Z., Tadé, M., Liu, S., 2019. Photo-driven bioelectrochemical photocathode with polydopamine-coated TiO_2 nanotubes for self-sustaining MoS_2 synthesis to facilitate hydrogen evolution. J. Power Sources 413, 310-317. https://doi.org/10.1016/j.jpowsour.2018.12.054.

Zhang, J., Wang, W., You, S., Qi, D., Liu, Z., Liu, D., Ma, M., Cui, F., Ren, N., Chen, X., 2020. Photothermal janus anode with photosynthesis-shielding effect for activating low-temperature biological wastewater treatment. Adv. Funct. Mater. 30 (7), 1909432. https://doi.org/10.1002/adfm.201909432.

Zhang, L., Álvarez-Martos, I., Vakurov, A., Ferapontova, E.E., 2017. Seawater operating bio-photovoltaic cells coupling semiconductor photoanodes and enzymatic biocathodes. Sustain. Energ. Fuels 1 (4), 842-850. https://doi.org/10.1039/C7SE00051K.

Zhang, T., 2015. More efficient together. Science 350 (6262), 738. https://doi.org/10.1126/science.aad6452.

Zhang, Y., He, Q., Xia, L., Li, Y., Song, S., 2018a. Algae cathode microbial fuel cells for cadmium removal with simultaneous electricity production using nickel foam/graphene electrode. Biochem. Eng. J. 138, 179-187. https://doi.org/10.1016/j.bej.2018.07.021.

Zhang, Y., He, Q., Xia, L., Li, Y., Song, S., 2018b. Algae cathode microbial fuel cells for cadmium removal with simultaneous electricity production using nickel foam/graphene electrode. Biochem Eng J 138, 179-187. https://doi.org/10.1016/j.bej.2018.07.021.

Zhou, D., Dong, S., Shi, J., Cui, X., Ki, D., Torres, C.I., Rittmann, B.E., 2017. Intimate coupling of an N-doped TiO_2 photocatalyst and anode respiring bacteria for enhancing 4-chlorophenol degradation and current generation. Chem. Eng. J. 317, 882-889. https://doi.org/10.1016/j.cej.2017.02.128.

Zhu, G., Yang, Y., Liu, J., Liu, F., Lu, A., He, W., 2017. Enhanced photocurrent production by the synergy of hematite nanowire-arrayed photoanode and bioengineered *Shewanella oneidensis* MR-1. Biosens. Bioelectron. 94, 227-234. https://doi.org/10.1016/j.bios.2017.03.006.

Declaration of interests

The authors declare that they have no known competing financial interests or personal relationships that could have appeared to influence the work reported in this paper.